ILLINOIS

UNIVERSITY OF ILLINOIS AT URBANA-CHAMPAIGN

-

PRODUCTION NOTE

University of Illinois at
Urbana-Champaign Library
Large-scale Digitization Project, 2007.

UNIVERSITY OF ILLINOIS
BULLETIN
Vol. 45 September 19, 1947 No. 8

ENGINEERING EXPERIMENT STATION
BULLETIN SERIES No. 369

STUDIES OF HIGHWAY SKEW SLAB-BRIDGES WITH CURBS

PART I: RESULTS OF ANALYSES

A REPORT OF AN INVESTIGATION
CONDUCTED BY
THE ENGINEERING EXPERIMENT STATION
UNIVERSITY OF ILLINOIS
IN COOPERATION WITH
THE PUBLIC ROADS ADMINISTRATION
FEDERAL WORKS AGENCY
AND
THE DIVISION OF HIGHWAYS
STATE OF ILLINOIS
BY

VERNON P. JENSEN
AND
JOHN W. ALLEN

PRICE: ONE DOLLAR

PUBLISHED BY THE UNIVERSITY OF ILLINOIS
URBANA

Published every five days by the University of Illinois. Entered as second-class matter at the post office at Urbana, Illinois, under the Act of August 24, 1912. Office of Publication, 358 Administration Building, Urbana, Illinois. Acceptance for mailing at the special rate of postage provided for in Section 1103, Act of October 3, 1917, authorized July 31, 1918.

THE Engineering Experiment Station was established by act of the Board of Trustees of the University of Illinois on December 8, 1903. It is the purpose of the Station to conduct investigations and make studies of importance to the engineering, manufacturing, railway, mining, and other industrial interests of the State.

The management of the Engineering Experiment Station is vested in an Executive Staff composed of the Director and his Assistant, the Heads of the several Departments in the College of Engineering, and the Professor of Chemical Engineering. This Staff is responsible for the establishment of general policies governing the work of the Station, including the approval of material for publication. All members of the teaching staff of the College are encouraged to engage in scientific research, either directly or in cooperation with the Research Corps, composed of full-time research assistants, research graduate assistants, and special investigators.

To render the results of its scientific investigations available to the public, the Engineering Experiment Station publishes and distributes a series of bulletins. Occasionally it publishes circulars of timely interest presenting information of importance, compiled from various sources which may not be readily accessible to the clientele of the Station, and reprints of articles appearing in the technical press written by members of the staff and others.

The volume and number at the top of the front cover page are merely arbitrary numbers and refer to the general publications of the University. *Above the title on the cover* is given the number of the Engineering Experiment Station bulletin, circular, or reprint which should be used in referring to these publications.

For copies of publications or for other information address

THE ENGINEERING EXPERIMENT STATION,
UNIVERSITY OF ILLINOIS,
URBANA, ILLINOIS

UNIVERSITY OF ILLINOIS
ENGINEERING EXPERIMENT STATION
BULLETIN SERIES No. 369

STUDIES OF HIGHWAY SKEW SLAB-BRIDGES WITH CURBS

PART I: RESULTS OF ANALYSES

A REPORT OF AN INVESTIGATION

CONDUCTED BY

THE ENGINEERING EXPERIMENT STATION
UNIVERSITY OF ILLINOIS

IN COOPERATION WITH

THE PUBLIC WORKS ADMINISTRATION
FEDERAL WORKS AGENCY

AND

THE DIVISION OF HIGHWAYS
STATE OF ILLINOIS

BY

VERNON P. JENSEN
FORMERLY RESEARCH ASSOCIATE PROFESSOR OF
THEORETICAL AND APPLIED MECHANICS

AND

JOHN W. ALLEN
FORMERLY SPECIAL RESEARCH GRADUATE ASSISTANT
IN THEORETICAL AND APPLIED MECHANICS

PUBLISHED BY THE UNIVERSITY OF ILLINOIS

4000—9-47—35003

UNIVERSITY
OF ILLINOIS
PRESS

ABSTRACT

This bulletin continues the studies being made of highway slab-bridges with curbs. Designs, and analyses, based on a difference equation method developed in Bulletin 332 are made for a range of bridges. Normal span lengths range up to about 30 ft., skew angles up to 60 deg. Only a single standard curb and handrail detail is considered in all designs. Tables and curves are given which show the variation of design moments with the bridge dimensions. These moments are compared with the corresponding moments in similar right slab-bridges with curbs, data on which have been given in Bulletin 315.

General features of the variations of design moments are discussed with a view toward incorporating, in the future, the results of this bulletin, together with the results of laboratory tests, into a simplified design procedure of a nature similar to that presented in Bulletin 346, which deals with simple span right bridges.

Data which have been used in the development of the results are presented in appendices.

This page is intentionally blank.

CONTENTS

LIST OF FIGURES

LIST OF TABLES

STUDIES OF HIGHWAY SKEW SLAB-BRIDGES WITH CURBS

PART I: RESULTS OF ANALYSES

I. Introduction

1. *Preliminary Remarks.*—This bulletin is a continuation of a previous one[1] dealing with skew slabs. In the earlier work, difference equations were set up from which deflections and moments could be determined in skew slab-bridges with curbs. These equations have been used in the present work to analyze a number of bridges having a roadway width of 24 ft. and having various spans and angles of skew. The results of the analyses are presented herein.

The method set forth in this bulletin is not to be construed as a final form of a design procedure. The bulletin is related to past and future publications on slab-bridges in that it continues the advance from the development of methods of analysis (Bulletins 315[2] and 332) toward the evolution of a final standard design procedure for skew slab-bridges. The principal object in this bulletin is to study analytically the effects of variations in bridge dimensions on quantities critical for design. The step next in order will be the testing of actual structures and the comparison of test results with analytical data.

Future publications will summarize the results of laboratory tests on one-half and one-fifth scale models of reinforced concrete skew slab-bridges with curbs, and will present a design procedure based on analyses and tests.

2. *Acknowledgments.*—The data contained herein were obtained by Mr. Allen for his thesis, which was submitted in 1941 in partial fulfillment of the requirements for the degree of Master of Science in Theoretical and Applied Mechanics in the Graduate School of the University of Illinois. The work was done in conjunction with the investigation of concentrated loads on reinforced concrete bridge slabs being conducted in the Engineering Experiment Station in cooperation with the Public Roads Administration of the Federal Works Agency and the Illinois Division of Highways.

The program of the investigation is guided by an Advisory Committee having the following personnel.

[1] V. P. Jensen, "Analyses of Skew Slabs." Univ. of Ill. Eng. Exp. Sta. Bul. 332, 1941. This bulletin contains references to earlier literature on skew slabs.

[2] V. P. Jensen, "Moments in Simple Span Bridge Slabs with Stiffened Edges," Univ. of Ill. Eng. Exp. Sta. Bul. 315, 1939.

Representing the Public Roads Administration:
E. F. KELLEY, Chief, Division of Physical Research
RAYMOND ARCHIBALD, Chief, Bridge Division.
Representing the Illinois Division of Highways:
G. F. BURCH, Bridge Engineer
L. E. PHILBROOK, Assistant Bridge Engineer (From 1936 until 1942 A. BENESCH, then Engineer of Grade Separations, served on the Advisory Committee).
Representing the University of Illinois:
F. E. RICHART, Research Professor of Engineering Materials
N. M. NEWMARK, Research Professor of Structural Engineering.
Consultants to the Committee, from the University of Illinois:
W. M. WILSON, Research Professor of Structural Engineering
T. C. SHEDD, Professor of Structural Engineering.

This bulletin was prepared for publication from Professor Jensen's preliminary manuscript by MYRON L. GOSSARD, Special Research Associate in Theoretical and Applied Mechanics, and Professor Newmark.

3. *Notation.*—The following notation is used:

w = deflection of slab, positive downward.
$w_1, w_2, \ldots$ = deflections of points 1, 2, ...
x, y = horizontal rectangular coordinate axes in the skew spanwise direction and perpendicular thereto, respectively.
r, s = horizontal rectangular coordinate axes in the normal spanwise direction and perpendicular thereto, respectively.
a = normal span length of bridge, measured between and perpendicular to the abutments.
b = width of bridge, measured between centers of, and perpendicular to, the curbs.
c = diameter of circular area over which a wheel load is assumed to be uniformly distributed.
$\lambda, \lambda_x, \lambda_y, \lambda_r, \lambda_s$ = distances, as defined in various figures, between points or lines of difference equation networks.
h = thickness of slab.
E = modulus of elasticity of the material of the slab.
E_1 = modulus of elasticity of the material of the curb or edge beam.
I_1 = moment of inertia of the cross-sectional area of a

curb or edge beam about its horizontal centroidal axis.

μ = Poisson's ratio of the material of the slab.

$N = \dfrac{Eh^3}{12(1-\mu^2)}$ = measure of stiffness of the slab.

$H = \dfrac{E_1 I_1}{aN}$ = dimensionless quantity defining the relative stiffness of curb or edge beam to slab.

$J = \dfrac{\lambda_y^3}{\lambda_x^3} \cdot \dfrac{E_1 I_1}{\lambda_x N}$ = dimensionless number proportional to the relative stiffness, H.

P = concentrated load, positive when acting downward.

p = distributed load on the slab per unit of area, positive when acting downward.

q = distributed load on a curb or edge beam per unit of length, positive when acting downward.

M_x and M_y or M_r and M_s = bending moments in the slab per unit of length, acting on sections normal to the x and y axes or to the r and s axes, respectively, positive when producing compression at the top.

M_{xy} or M_{rs} = twisting moment in the slab per unit of length, acting on sections normal to the x and y axes or to the r and s axes, respectively, positive when producing compression at the top in the direction of the line $x=y$ or the line $r=s$, respectively.

M_{or} or M_{os} = modified bending moment per unit of length in the r or s direction, respectively, in a simply supported slab of infinite length, and beneath a load at the center uniformly distributed over a small circular area. Such moments, when used in the ordinary theory of flexure, give stresses at the bottom of the slab approximately equal to those obtained from the more exact thick-slab theory.

M_{cor} = corrective bending moment in the slab per unit of length, beneath a load uniformly distributed over a small circular area, to be applied to a difference equation solution.

M_{curb} = bending moment in a curb or edge beam, positive when producing compression at the top.

θ_x = angle of inclination, with respect to the x-axis, of the direction of maximum bending moment in the slab.

II. Analyses of Skew Slab-Bridges

4. *Theoretical Basis for Analyses.*—The derivations of the difference equations for analyzing the slabs are described in detail in Bulletin 332, Chapters II and IV. Neither the derivations nor the equations themselves are repeated here. It is sufficient to state that the usual assumptions are made that the slab is of homogeneous, isotropic, and elastic material and is of constant thickness. The curb is assumed to act in the manner of an edge beam of stiffness E_1I_1 attached to the slab in such a way as to undergo the same deflection as the edge of the slab and to transmit only vertical reactions to the slab at its edge.

The difference equations used in the analysis are the difference analogs of the corresponding well-known differential equations pertaining to the analysis of slabs. Their use reduces the problem from one of an infinite degree of indeterminateness to one of a finite degree by confining attention to a finite number of points on the slab. These points are chosen as the intersections of a regularly spaced network of crossing lines on the slab.

Some approximation is introduced by the substitution of the difference analogs for the differential equations. The percentage of error in the bending moments reduces with the closeness of the points of the network and, in general, increases with the sharpness of variation of the moments. The sharpest variation of moments occurs directly under a concentrated load. Through the introduction of a corrective term, however, the bending moments directly under a wheel load on the bridge are represented with reasonable accuracy.

A considerable number of factors influence the distribution of moments in a skew slab-bridge. Among these are the following: ratio of width to span; angle of skew; relative stiffness of curb and slab; spacing and magnitudes of wheel loads; permissible unit stresses.* The present studies are not intended to cover all possible variations of all these factors. They are limited in general to a consideration of the two-lane bridge having a roadway width of approximately 24 ft. Angles of skew up to 60 degrees are considered. Spans are limited, in general, to a maximum of 30 ft. measured normal to the abutments, although one bridge having a span of almost 36 ft. is analyzed. Designs are based on the 1935 specifications of the American Association of State Highway Officials†; therefore, HS truck loadings are not con-

* Permissible unit stresses influence the distribution of moments only by determining the controlling dimensions.

† Hereinafter referred to as the AASHO.

sidered. As far as practicable, a single curb detail, adopted as standard for these studies, was adhered to. Because tests[3] have shown that the slab-bridge is capable of sustaining relatively high loads before failure, working stresses were adopted as follows:

f_c = allowable concrete stress = 1000 p.s.i.
f_s = allowable steel stress = 20,000 p.s.i.
n = ratio of moduli, E_s/E_c = 12.

Although the foregoing limitations apply in general to the results presented herein, certain departures from them are permissible; these are indicated in the detailed discussions of the various curves of bending moment.

Figure 1 shows plans of the various bridges analyzed by difference equations. Supplemental data for each bridge are given in Table 1. In addition, a number of bridges of short span were studied by the application of coefficients given in Bulletin 315 and by an influence surface for the infinite strip slab.[4] While these coefficients were determined for a right bridge (zero-degree skew), they apply to the central region of a skew bridge of small normal span and relatively large width.

5. *Computation Procedure.*—The procedure described in this section for analyzing a typical bridge is considered to be a tool for research. It is not recommended for general use in an office for the design of skew slab-bridges, although it has perfectly general applicability to such bridges of any proportion, angle of skew, or loading. The method is recommended for special investigations. The analytical procedure is used herein to furnish an understanding of the behavior of particular skew slab-bridges and to provide curves of moment from which a simplified design procedure may be evolved.

For the purpose of the investigation reported in this bulletin, the width of roadway was held constant, whereas the angle of skew and the normal span were permitted to vary. Thus, for each arbitrary angle of skew an attempt was made to analyze a range of spans up

[3] See for example V. P. Jensen, R. W. Kluge, and C. B. Williams, Jr., "Highway Slab-Bridges with Curbs: Laboratory Tests and Proposed Design Method," Univ. of Ill. Eng. Exp. Sta. Bul. 346, Table 5, p. 44. 1943.

[4] H. M. Westergaard, "Computation of Stresses in Bridge Slabs Due to Wheel Loads," Public Roads, Vol. 11, No. 1, p. 15. March, 1930.

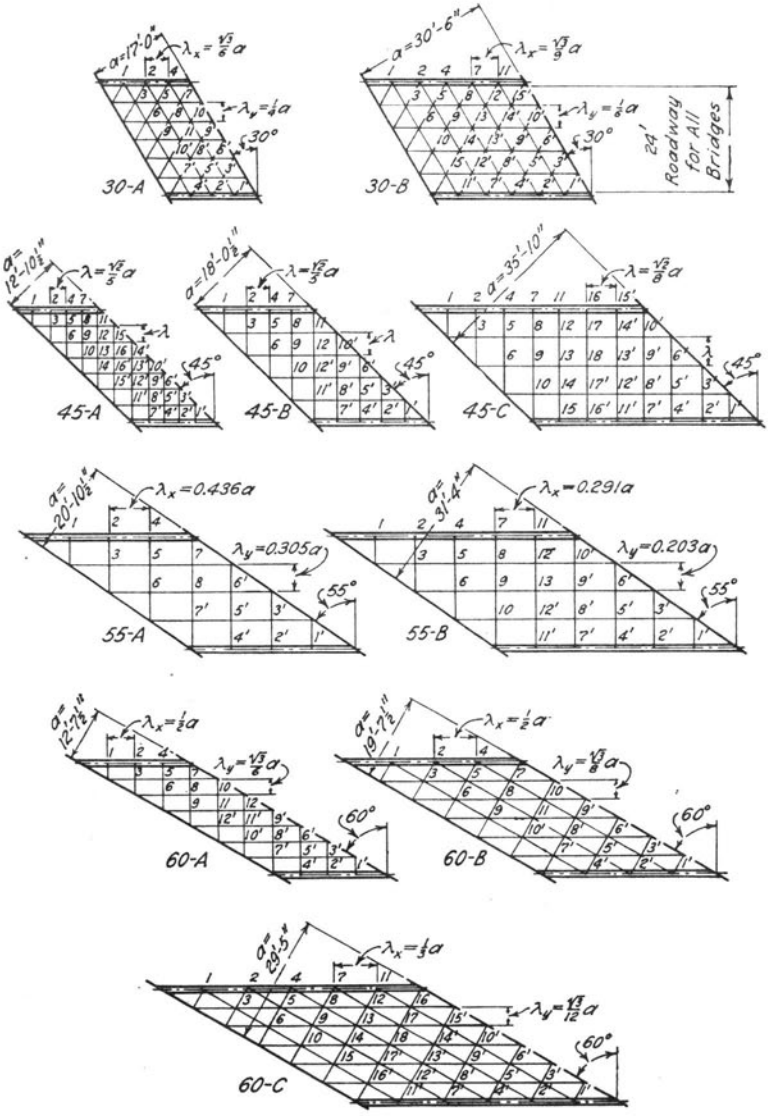

FIG. 1. PLANS OF SKEW SLAB-BRIDGES ANALYZED BY DIFFERENCE EQUATIONS, SHOWING NETWORKS USED

TABLE 1

DATA USED IN ANALYSES OF SKEW SLAB-BRIDGES

Clear width of roadway is 24 ft. for all bridges. b = width center to center of curbs, approximately 25 ft. 6 in. Stiffness factors, H and J, are defined in Section 3.

Slab No.	Angle of Skew deg.	Normal Span, a ft.	Ratio of Width to Normal Span b/a	Total Thickness of Slab in.	$J = \left(\frac{\lambda_y}{\lambda_x}\right)^3 \frac{E_1 I_1}{\lambda_x N}$	$H = \frac{E_1 I_1}{aN}$	Uniform Dead Load, p* lb./ft.^{2}	Weight of Curb and Handrail, q lb./ft.	Rear Wheel Load with Impact, P† lb.	Diam. of Equivalent Circular Loaded Area c‡	Corrective Moment under Wheel, M_{cor}‡¶ $(P=1)$
(1)	(2)	(3)	(4)	(5)	(6)	(7)	(8)	(9)	(10)	(11)	(12)
30-A	30	17.00	1.50	13	1.30	0.58	187	480	21 630	$0.59\,\lambda_y$	0.057
30-B	30	30.5	0.83	19	0.66	0.194	263	568	21 150	$0.59\,\lambda_y$	0.055
45-A	45	12.88	1.98	11.5	3.00	0.85	169	475	.....	.....	.....
45-B	45	18.04	1.41	13.5	1.50	0.424	194	495	21 600	$0.70\,\lambda$	0.092
45-C	45	35.8	0.71	24	1.00	0.177	325	697	20 970	$0.70\,\lambda$	0.080
55-A	55	20.9	1.22	14	0.33	0.417	200	526	.....	.....	.....
55-B	55	31.3	0.81	22	0.20	0.17	300	621	.....	.....	.....
60-A	60	12.63	2.02	11.5	0.33	0.87	169	472	.....	.....	.....
60-B	60	19.63	1.30	14	0.065	0.40	200	506	21 500	$c_r = 0.78\,\lambda_r$ $c_s = 0.88\,\lambda_r$	(r) 0.096 (s) 0.108
60-C	60	29.4	0.87	22	0.046	0.189	300	595	21 200	$c_r = 0.78\,\lambda_r$ $c_s = 0.88\,\lambda_r$	(r) 0.079 (s) 0.091

* Uniform dead load includes paving allowance of 25 lb./ft.^{2}

† Impact factor is taken as $I = \frac{50 \text{ ft.}}{125 \text{ ft.} + \text{Normal Span}}$.

‡ See Bulletin 332, Sections 12 and 14, and Appendix A of this bulletin.

¶ Corrective moment in direction r is normal to supports and in direction s is parallel to supports. These differ because of the rectangularity of the network. Corrective moment is for a circular loaded area of 1.25 ft. diameter.

to at least 30 ft. It was possible to choose such spans as would permit the use of convenient networks of squares, rectangles, or equilateral triangles. Equations pertaining to slabs having various networks are given in Bulletin 332.

The procedure to be followed in making an investigation may then be outlined as follows:

1. Select the dimensions of the bridge and the network. Skew — arbitrary. Width (fixed by width of roadway and curb details)—about 25 ft. 6 in. for all bridges studied. Span (variable, to suit network of points) — range up to 30 ft.

2. Estimate the required thickness of slab, h, and compute the value of J, where

$$J = \frac{\lambda_y^3}{\lambda_x^3} \cdot \frac{E_1 I_1}{\lambda_x N}.$$

3. Select from Bulletin 332 the equations appropriate to the given type of network and compute the values of the constants which appear in the equations.

4. Determine influence surfaces for moments at or near the center of the slab and for moment near the center of the curb. Details are given in Bulletin 332.

5. Analyze the bridge for dead load, either by the influence surfaces or by solving simultaneous equations for deflections and computing moments according to the appropriate equations given in Bulletin 332.

6. By spotting truck wheel loads at various positions on the bridge and by using the previously determined influence ordinates, obtain curves from which the maximum moments in the slab and the curb may be determined.

7. From the calculated dead and live load moments, check the required thickness of slab.

8. If the required thickness of slab differs considerably from the assumed value, follow one of three procedures: (a) recompute the value of J and modify the moments by estimation to take approximate account of the changed relative stiffness of curb; (b) change the detail of curb to provide the relative stiffness required by the initial value of J; (c) re-analyze the bridge, using a corrected value for the thickness of slab and a new value of J.

The various steps are illustrated in somewhat more detail in their application to slab 30-B. Numerical data for this bridge are summarized on the Computation Sheet.

Computation Sheet

Data for slab 30-B

Angle of skew ..... = 30 deg.
Normal span (a) ..... = 30 ft. 6 in.
Center to center of curbs (b) ..... = 25 ft. 5 in.
b/a ratio ..... = 0.83

$$\lambda_y = \frac{\sqrt{3}}{2} \cdot \lambda_x = \frac{a}{6} \quad \ldots\ldots = 5.08 \text{ ft.}$$

$$J = \frac{\lambda_y^3}{\lambda_x^3} \cdot \frac{E_1 I_1}{\lambda_x N} = \left(\frac{3\sqrt{3}}{8}\right) \frac{17}{70.3} \left(\frac{31}{19}\right)^3 0.96 \cong 0.66$$

$$H = \frac{E_1 I_1}{aN} = \frac{17}{366} \left(\frac{31}{19}\right)^3 0.96 \quad \ldots\ldots \cong 0.194$$

$$p = \frac{19}{12}(150) + 25 \text{ (paving)} \quad \ldots\ldots = 263 \text{ lb./ft.}^2$$

Area of curb* = 6 (9) ..... = 54 sq. in.
11 (12) ..... = 132
19 (8.5) ..... = 162
Area of handrail ..... = 197
545 sq. in.

$$q = \text{edge load} = \frac{150}{144}(545) = 568 \text{ lb./ft.}$$

$$q/\lambda_y = \frac{568}{5.08\,(263)}\, p = 0.425p.$$

Live load (H-20 truck loading)

$$\text{Impact}\dagger = \frac{50}{125 + 30.5} \quad \ldots\ldots = 0.321$$

Rear wheel = 16,000 (1.321) ..... = 21,150 lb.
Front wheel = 4,000 (1.321) ..... = 5,290 lb.

Corrective moment for point 13 in slab for loaded area of 1.25 ft.
Assume $c = 0.59\lambda_y = 3.00$ ft. (See Appendix A)

$$M_{cor} = \frac{P}{2.32 + 8\dfrac{1.25}{30.5}} - \frac{P}{2.32 + 8\dfrac{3.00}{30.5}} = 0.055P.$$

* In computing the weight of a curb, the boundary between curb and slab is considered to be that indicated by the dashed line in the curb detail of Fig. 2. A procedure more consistent with the definition of curb as used in calculations of curb stiffness would be to consider the junction of curb and slab to be at the plane tangent to the inside face of curb. However, the total dead load effect of curbs and slab combined is independent of the definition of junction of curb and slab. The procedure illustrated is followed consistently throughout this bulletin.

† The 1935 specification of the AASHO places no upper limit on the impact factor.

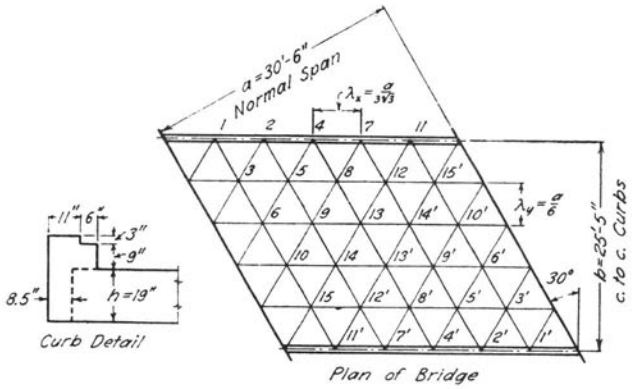

FIG. 2. PLAN AND DETAIL OF SKEW SLAB-BRIDGE 30-B

Step 1. The dimensions of this bridge and the form of the network are shown in Fig. 2. Since the angle of skew is 30 deg. it is logical to use a network of equilateral triangles and to adjust the span so that the abutments coincide with lines of the network as shown in the figure. The numbers on the points of the network indicate that 15 simultaneous equations must be solved for each symmetrical or antisymmetrical loading considered.

Step 2. The required slab thickness was estimated from the moment in a right bridge of identical normal span and width of roadway. For slab 30-B the estimated over-all depth was 19 in. For this depth of slab the value of the constant J was determined to be approximately 0.66, as indicated on the Computation Sheet.

Step 3. The equations appropriate to a network of equilateral triangles are given in Bulletin 332, Section 8, Equations (98) through (106). For Poisson's ratio μ of 0.2 and for $J = 0.66$, the coefficients of the deflections in these equations take simple numerical values. Applied to slab 30-B, Fig. 2, the equations become:

For symmetrical loading: $(w_n = w_{n'})$

$$\frac{2p_1\lambda_y^4}{N} + \frac{4q_1\lambda_y^3}{N} = 25\,w_1 - 16.28\,w_2 - 7.2\,w_3 + 3.12\,w_4 + 2.2\,w_5 + w_6.$$

$$\frac{2p_2\lambda_y^4}{N} + \frac{4q_2\lambda_y^3}{N} = -16.28\,w_1 + 30.32\,w_2 - 6.2\,w_3 - 16.28\,w_4 - 6.2\,w_5 + 2\,w_6 + 3.12\,w_7 + 2.2\,w_8 + w_9.$$

$$\frac{4p_3\lambda_y^4}{N} = -7.2\,w_1 - 6.2\,w_2 + 38\,w_3 + 2.2\,w_4 - 11\,w_5 - 11\,w_6 + w_8 + 2\,w_9 + w_{10}.$$

$$\frac{2p_4\lambda_y^4}{N} + \frac{4q_4\lambda_y^4}{N} = 3.12\,w_1 - 16.28\,w_2 + 2.2\,w_3 + 30.32\,w_4 - 6.2\,w_5 + w_6 - 16.28\,w_7 - 6.2\,w_8 + 2\,w_9 + 3.12\,w_{11} + 2.2\,w_{12} + w_{13}.$$

$$\frac{4p_5\lambda_y^4}{N} = 2.2\,w_1 - 6.2\,w_2 - 11\,w_3 - 6.2\,w_4 + 40\,w_5 - 10\,w_6 + 2.2\,w_7 - 11\,w_8 - 10\,w_9 + 2\,w_{10} + w_{12} + 2\,w_{13} + w_{14}.$$

$$\frac{4p_6\lambda_y^4}{N} = w_1 + 2\,w_2 - 11\,w_3 + w_4 - 10\,w_5 + 40\,w_6 + 2\,w_8 - 10\,w_9 - 11\,w_{10} + w_{13} + 2\,w_{14} + w_{15}.$$

$$\frac{2p_7\lambda_y^4}{N} + \frac{4q_7\lambda_y^3}{N} = 3.12\,w_2 - 16.28\,w_4 + 2.2\,w_5 + 30.32\,w_7 - 6.2\,w_8 + w_9 - 16.28\,w_{11} - 6.2\,w_{12} + 2\,w_{13} + w_{14} + 2.2\,w_{15}.$$

$$\frac{4p_8\lambda_y^4}{N} = 2.2\,w_2 + w_3 - 6.2\,w_4 - 11\,w_5 + 2\,w_6 - 6.2\,w_7 + 40\,w_8 - 10\,w_9 + w_{10} + 2.2\,w_{11} - 11\,w_{12} - 9\,w_{13} + 4\,w_{14} + w_{15}.$$

$$\frac{4p_9\lambda_y^4}{N} = w_2 + 2\,w_3 + 2\,w_4 - 10\,w_5 - 10\,w_6 + w_7 - 10\,w_8 + 42\,w_9 - 10\,w_{10} + 3\,w_{12} - 8\,w_{13} - 9\,w_{14} + 2\,w_{15}.$$

$$\frac{4p_{10}\lambda_y^4}{N} = w_3 + 2\,w_5 - 11\,w_6 + w_8 - 10\,w_9 + 40\,w_{10} + w_{11} + 2\,w_{12} + 3\,w_{13} - 10\,w_{14} - 11\,w_{15}.$$

$$\frac{2p_{11}\lambda_y^4}{N} + \frac{4q_{11}\lambda_y^3}{N} = +3.12\,w_4 - 16.28\,w_7 + 2.2\,w_8 + w_{10} + 28.40\,w_{11} - 6.2\,w_{12} + w_{13} + 2\,w_{14} - 7.4\,w_{15}.$$

$$\frac{4p_{12}\lambda_y^4}{N} = 2.2\,w_4 + w_5 - 6.2\,w_7 - 11\,w_8 + 3\,w_9 + 2\,w_{10} - 6.2\,w_{11} + 40\,w_{12} - 8\,w_{13} - 9\,w_{14} - 11\,w_{15}.$$

$$\frac{4p_{13}\lambda_y^4}{N} = w_4 + 2w_5 + w_6 + 2\,w_7 - 9\,w_8 - 8\,w_9 + 3\,w_{10} + w_{11} - 8\,w_{12} + 32\,w_{13} - 20\,w_{14} + 3\,w_{15}.$$

$$\frac{4p_{14}\lambda_y^4}{N} = w_5 + 2\,w_6 + w_7 + 4\,w_8 - 9\,w_9 - 10\,w_{10} + 2\,w_{11} - 9\,w_{12} - 20\,w_{13} + 44\,w_{14} - 10\,w_{15}.$$

$$\frac{4p_{15}\lambda_y^4}{N} = w_6 + 2.2\,w_7 + w_8 + 2\,w_9 - 11\,w_{10} - 7.4\,w_{11} - 11\,w_{12} + 3\,w_{13} - 10\,w_{14} + 39\,w_{15}.$$

For anti-symmetrical loading ($w_{n'} = -w_n$) the first six equations remain unchanged, but the rest have certain of their coefficients altered. Since these are easily obtained from the general equations, they are not stated here.

The intensity of loading at each point remains to be specified for each type of loading.

Step 4. The influence surfaces for M_x, M_y, and M_{xy} at point 13 may be obtained from applications of Newmark's theorem.[5]

Theorem: Where a particular effect Q is a linear function of the deflections $w_a, w_b, \ldots, w_k$ at points $a, b, \ldots, k$, respectively, as in the equation

$$Q = Aw_a + Bw_b + \ldots + Kw_k,$$

and if deflections and loads are linearly related, the influence on Q of a unit load at any point m is obtained as the deflection at the point m due to loads of magnitude $A, B, \ldots, K$, applied at points $a, b, \ldots, k$, respectively.

Applications of this theorem are described in Bulletin 332, Chapter IV.

To illustrate the application of the theorem to slab 30-B it is sufficient to consider the influence surface for M_x at point 13. The equation for M_x at point 13 is, according to Equation (107) of Bulletin 332,

$$(M_x)_{13} = \frac{N}{4\lambda_y^2}\left[6\,(1+\mu)\,w_{13} - (3-\mu)\,(w_9 + w_{14'}) - 2\mu\,(w_8 + w_{12} + w_{14} + w_{13'})\right]. \qquad (1)$$

The theorem therefore permits the moment M_x at point 13 due to a unit load at any point m to be found as the deflection of point m due to loads

$$\left.\begin{aligned} P_{13} &= \frac{6\,(1+\mu)\,N}{4\lambda_y^2}, \qquad P_9 = P_{14'} = -\frac{(3-\mu)\,N}{4\lambda_y^2}, \\ P_8 &= P_{12} = P_{14} = P_{13'} = -\frac{2\mu\,N}{4\lambda_y^2} \end{aligned}\right\}. \qquad (2)$$

That is, the deflection of the slab due to these loads is the influence surface for M_x at point 13.

Since the set of loads does not possess point symmetry with respect to the center of the slab, it is broken into two sets, one sym-

[5] N. M. Newmark, "Note on the Calculation of Influence Surfaces in Plates by Use of Difference Equations," Jour. Applied Mech., Am. Soc. Mech. Eng., Vol. 8, No. 2, p. A-92, June, 1941.

metrical and one anti-symmetrical, whose sum is given by Equation (2). In the symmetrical system the loads are

$$\left.\begin{aligned} P_{13} = P_{13'} = (3+2\mu)\frac{N}{4\lambda_y^2}, \quad P_9 = P_{9'} = -\frac{(3-\mu)}{2}\cdot\frac{N}{4\lambda_y^2}, \\ P_8 = P_{8'} = P_{12} = P_{12'} = -\mu\frac{N}{4\lambda_y^2}, \quad P_{14} = P_{14'} = -\frac{(3+\mu)}{2}\cdot\frac{N}{4\lambda_y^2} \end{aligned}\right\}. \quad (3)$$

These magnitudes of the loads may be substituted into the left sides of the simultaneous equations. It is assumed that, at any point n, the distributed load p_n is related to P_n as follows:

$$p_n = \frac{P_n}{\lambda_x \lambda_y} = \frac{\sqrt{3}}{2}\cdot\frac{P_n}{\lambda_y^2}. \quad (4)$$

The loads at points 1 to 7 inclusive and at points 10, 11, and 15 are zero.

The anti-symmetrical loads corresponding to (3) are

$$\left.\begin{aligned} P_{13} = -P_{13'} = (3+4\mu)\frac{N}{4\lambda_y^2}, \quad P_9 = -P_{9'} = -\frac{(3-\mu)}{2}\cdot\frac{N}{4\lambda_y^2}, \\ P_8 = -P_{8'} = P_{12} = -P_{12'} = -\mu\frac{N}{4\lambda_y^2}, \quad P_{14} = -P_{14'} = \frac{3(1-\mu)}{2}\cdot\frac{N}{4\lambda_y^2} \end{aligned}\right\}. \quad (5)$$

These, reduced to distributed loads by means of Equation (4), must be substituted into the equations for anti-symmetrical loading. The sums of the deflections due to the two systems of loads represent the influence ordinates for moment M_x at point 13.

Similarly the influence ordinates for moments M_y and M_{xy} at point 13 and for M_{curb} at points 4 and 7 may be obtained. As a matter of fact, in the solution of a system of equations for symmetrical or for anti-symmetrical deflections, any number of sets of loads may be handled at the same time. Each new set of loads merely adds a column to the tabulated calculations of the type described in Bulletin 332, Appendix A.

The bending moments in a slab under a load distributed over a small area are affected by the degree of concentration of the load. Except for the region over which the load is applied, the effect is negligible. In general the moments at the load point need special

consideration. Therefore, a correction must be made to the influence ordinates for M_x and M_y at point 13 as determined from the difference equation analysis. The manner of determining the correction for a square network of points was described in detail in Bulletin 332, Sections 12 and 14. Stated briefly, the determination of the correction has the following basis.

The influence ordinates for M_x and M_y at point 13 due to $P_{13}=1$ which result from a difference equation analysis would be consistent with the respective influence ordinates determined by an exact analysis (if such were possible) provided that the load were distributed over some area of diameter c. If the value of c is known (it can be calculated approximately for all slab networks), each of the moments may be corrected for another diameter of loaded area, c_1, by the addition of a correction

$$\left(M_{cor}\right)_{13}^{P_{13}=1} = \frac{1}{2.32 + 8\frac{c_1}{a}} - \frac{1}{2.32 + 8\frac{c}{a}}, \qquad (6)$$

wherein a is the normal span of the slab. Equation (6) is based upon Westergaard's approximate equation[6] for the effect of load concentration at the center of an infinitely long slab.

For the purpose of this investigation, c_1 was always made equal to 1.25 ft. The diameter c, which is seen to be tacitly assumed in all difference equation analyses, depends upon the shape and fineness of the network used in the calculations. For the square networks which have been used it was shown in Bulletin 332 that a reasonable value of c is given by the equation

$$c = 0.70\lambda,$$

where λ is the distance between successive points of the network.

For the hexagonal network used for slab 30-B it is shown in Appendix A that a reasonable value of c is given by the equation

$$c = 0.59\lambda_y.$$

Since $\lambda_y = a/6$ for slab 30-B,

$$c = 0.59\frac{a}{6},$$

and, from Equation (6), the correction to the influence ordinates M_x

[6] H. M. Westergaard, "Computation of Stresses in Bridge Slabs Due to Wheel Loads," Public Roads, Vol. 11, No. 1, p. 10, Equation (66), March, 1930.

and M_y at point 13 is

$$\left(M_{cor}\right)_{13}^{P_{11}=1} = 0.055,$$

as shown on the Computation Sheet. For slab 30-B as well as for the other slabs analyzed, the corrected influence ordinates are given in the tables in Appendix B.

Contours on the influence surfaces were drawn according to the ordinates at the points of the network. Points on the contour lines were taken from profiles of the influence surfaces. Contours on the influence surfaces for slab 30-B are shown in Fig. 16 in Appendix B.

Step 5. The dead loads to be considered include the weight of the slab, curb, and handrail plus any pavement allowance required by the specifications. The weight of the slab and the pavement allowance are added in order to obtain the intensity of loading, p, which is constant for all points of the network. It is convenient to express q, the weight per unit length of curb and handrail, in terms of p and λ_y. For slab 30-B, on the Computation Sheet,

$$p = 263 \text{ lb./ft.}^2$$

$$q = 568 \text{ lb./ft.},$$

including the weight of a concrete handrail and concrete spindles, and

$$\frac{q}{\lambda_y} = 0.425p.$$

The loading terms in the simultaneous equations given in Step 3 then take either of the forms

$$\frac{2p_n\lambda_y^4}{N} + \frac{4q_n\lambda_y^3}{N} = \frac{4p\lambda_y^4}{N}\left(\frac{1}{2} + 0.425\right) = 0.925\frac{4p\lambda_y^4}{N} = 0.925C,$$

or, for the terms without edge load,

$$\frac{4p_n\lambda_y^4}{N} = \frac{4p\lambda_y^4}{N} = C.$$

Deflections of the slab in terms of the factor C are then determined from the simultaneous equations. From these deflections the bending moments may be obtained from Equations (107) through (110) of Bulletin 332. The most significant moments are those at point 13 on the center line of the normal span.

Step 6. Truck wheel loads were placed on the influence surfaces to obtain the positions of the trucks for the greatest moments at the various points under consideration. The maximum moment at a given point in the curbs due to the truck loadings was found by placing the trucks on the influence surface for moment at the given point. The trucks were placed on lane spacings as shown in Fig. 16. The influence ordinate at the position of each wheel was multiplied by the wheel load to get the moment at the critical section. The moment in the curb was found for each truck separately, since their effects are independent and superposable. Each truck was permitted to occupy different positions on its lane of traffic, a value of moment being obtained for each position. The final positions of the trucks for maximum moment in the curb were obtained from plotted curves of moment. These positions are shown on the influence surfaces, Fig. 16.

The determination of the greatest live load moment at point 13 involves M_x, M_y, and M_{xy}, since

$$M_{\max} = \frac{M_x + M_y}{2} + \sqrt{\left(\frac{M_x - M_y}{2}\right)^2 + M^2_{xy}}\,.$$

The position of the truck in one lane must be such that a rear wheel is over point 13. The truck in the other lane must be placed in succession at several positions. For each position M_x, M_y, M_{xy}, and $M_{\max}$ due to *both* trucks must be computed. From a plotted curve of $M_{\max}$ with position of truck the final position of truck and the greatest value of $M_{\max}$ due to live load may be obtained.

The maximum moment makes an angle θ_x with the x-axis, where

$$\theta_x = \frac{1}{2}\tan^{-1}\frac{2M_{xy}}{M_x - M_y}\,.$$

It will usually be found that at a point near the center of the slab the directions of maximum live load and dead load moments differ from one another by only a few degrees. For this reason the maximum live and dead load moments may merely be added to obtain the design moment. If these directions differed considerably it would be necessary, when determining a curve of $M_{\max}$ to give the greatest combined effect, to include M_x, M_y, and M_{xy} due to dead load with the corresponding moments due to the two trucks.

For slab 30-B the greatest live and dead load moments in the slab and in the curb are given in Tables 2 and 3.

TABLE 2
SUMMARY OF DEAD LOAD MOMENTS

All bridges are of 24 ft. roadway.
b = distance center to center of curbs, nominally 25 ft. 6 in.

Slab No.	Ratio of Sides, b/a	Relative Stiffness of Curb, H	Dead Load Moments					
			Curb		Center of Slab			
			$\frac{M_{max}}{pa^2}$	$\frac{M_{skew}-M_{rt}}{M_{rt}}$ in percent	$\frac{M_{max}}{pa^2}$	$\frac{M_{skew}-M_{rt}}{M_{rt}}$ in percent	θ_x deg.	$\frac{M_{min}}{pa^2}$
(1)	(2)	(3)	(4)	(5)	(6)	(7)	(8)	(9)
30-A	1.50	0.58	0.0462	6.5	0.112	8.7	30	0.027
R30-A	1.50	0.58	0.0434		0.103		0	0.027
30-B	0.83	0.194	0.0198	0.0	0.115	15.0	26.5	0.011
R30-B	0.83	0.194	0.0198		0.100		0	0.026
45-A	1.98	0.85	0.0718	31.0	0.122	8.9	45	0.026
R45-A	1.98	0.85	0.0548		0.112		0	0.030
45-B	1.41	0.424	0.0421	17.9	0.122	15.1	45	0.023
R45-B	1.41	0.424	0.0357		0.106		0	0.032
45-C	0.71	0.177	0.0186	8.1	0.138	42.2	35	−0.011
R45-C	0.71	0.177	0.0172		0.097		0	0.023
55-A	1.22	0.417	0.0430	26.5	0.137	35.6	54.5	0.008
R55-A	1.22	0.417	0.0340		0.101		0	0.032
55-B	0.81	0.17	0.0183	5.8	0.162	58.8	43.5	−0.030
R55-B	0.81	0.17	0.0173		0.102		0	0.025
60-A	2.02	0.87	0.0926	66.5	0.122	8.9	60.5	0.027
R60-A	2.02	0.87	0.0556		0.112		0	0.029
60-B	1.30	0.40	0.0445	33.2	0.144	38.5	57	0.002
R60-B	1.30	0.40	0.0334		0.104		0	0.033
60-C	0.87	0.189	0.0208	8.9	0.181	75.7	48	−0.048
R60-C	0.87	0.189	0.0191		0.103		0	0.026

Step 7. The greatest moments in the slab at point 13, as given in Tables 2 and 3, are

$$M_{max}\ (\text{live load}) = 22{,}900 \text{ ft. lb. per ft.}$$

$$M_{max}\ (\text{dead load}) = 0.115\ pa^2$$

$$= 0.115\ (263)\ (30.5)^2$$

$$= 28{,}100 \text{ ft. lb. per ft.}$$

The directions of these moments differ by about 1½ deg.; this difference is of no practical importance. The moments may therefore be added directly, giving

$$M_{max}\ (\text{total load}) = 51{,}000 \text{ ft. lb. per ft.}$$

TABLE 3
SUMMARY OF LIVE LOAD MOMENTS
All bridges are of 24 ft. roadway.
b = distance center to center of curbs, nominally 25 ft. 6 in.

Slab No.	Live Load Moments						
	Curb		Center of Slab				Blunt Corner
	M_{max} ft.-lbs.	$\frac{M_{skew}-M_{rt}}{M_{rt}}$ in percent	M_{max} ft.-lbs./ft.	$\frac{M_{skew}-M_{rt}}{M_{rt}}$ in percent	θ_s deg.	M_{min}* ft.-lbs./ft.	Max. Neg. Mom. ft.-lbs./ft.
(1)	(2)	(3)	(4)	(5)	(6)	(7)	(8)
30-A	65 900	−2.8	14 100	−3.2	25.5	7210	
R30-A	67 800		14 550		0	6700	
30-B	109 500	7.9	22 900	7.0	25	7820	3520 (Pt. 15)
R30-B	101 500		21 400		0	8140	
45-B	66 000	2.8	13 970	−9.3	45	9210	
R45-B	64 200		15 400		0	6800	
45-C	138 700	6.7	27 180	13.0	30.5	7550	
R45-C	130 000		24 050		0	8250	
60-B	67 500	−4.6	14 800	−7.8	57.5	8020	3910 (Pt. 7)
R60-B	70 700		16 050		0	7100	
60-C	89 900	−2.3	21 850	2.1	46	6460	7940 (Pt. 16)
R60-C	92 000		21 400		0	7910	

* These are minimum moments which occur for wheel loads placed to produce maximum moments at center of slab.

For this moment the required slab thickness is

$$D = 1.5 + d = 1.5 + \sqrt{\frac{51{,}000}{164}} = 1.5 + 17.7 = 19.2 \text{ in.}$$

In this instance the assumed thickness of 19 in. recorded in Table 1 is satisfactory.

Step 8. No modification of moments or of curb size is required for slab 30-B; for other slabs, the dimensions of the curbs were changed slightly to fit the analyses. However, in the curves of dead load moment (Figs. 4, 8, and 11), the results for the skew bridges have been adjusted (by an estimate based on the effect of varying the curb stiffness in right bridges) to values which may be expected with standard curbs.

Some modification of the procedure indicated in the preceding steps may be necessary in particular instances. For example, in the determination of the maximum moment in the curb it is known that the maximum dead load moment does not occur at exactly the mid-point of the span, but rather shifts somewhat toward the obtuse

corner of the slab. From the nature of the procedure and the limitations of the difference equations, the moments can be found at only the few points of the network along the curb. The values at these few points were considered to give a satisfactory indication of the maximum moment in the curb of slab 30-B. However, in slabs 55-A, 60-A, and 60-B it was necessary to interpolate between points to obtain the maximum moment. The method used for the interpolation was to fit an equation

$$M = A + Bx + Cx^2 + Dx^3$$

to the curve of moments so that it gave the moment in the curb at four adjacent points. The maximum ordinate to the curve was determined by differentiation in the usual manner.

For comparison with the moments found in the analysis of the skew bridges, moments in comparative right bridges having identical normal spans, identical width of roadway, identical values of H, and identical values of q/pa were obtained from the curves and tables of Bulletin 315. It should be noted that the comparative right bridges are not so designed as to have the proper working stresses; instead, each has the same numerical values of b, a, H, and q/pa as the corresponding skew bridge. In the tables, curves, and text of this bulletin, the comparative right bridge for any skew bridge is designated by the same symbol as the skew bridge, prefixed by the letter R. However, a designed right bridge, for which numerical coefficients are given in some of the figures, is designated as a bridge of zero-degree skew. There is in general a slight difference between a bridge such as R30-B and a bridge of zero-degree skew having the same value of b/a. All correction factors for the determination of moments in skew bridges are based on the comparative (R) right bridge values and not on the values for the designed bridges of zero-degree skew.

The Gauss-Doolittle method of successive substitution, described in Appendix A of Bulletin 332, was used in the solution of all sets of simultaneous equations. The merit of the method is demonstrated by the fact that, with some experience, about 20 hours is sufficient to solve simultaneous equations for three systems of loadings. A calculating machine was used in this work.

6. *Numerical Results of Analyses.*—Data for the numerical calculations are given in Table 1 for the various skew bridges analyzed. Column 1 gives the slab designation and column 2 the angle of skew. For each angle of skew several spans were investigated, as indicated

in column 3. Since the width of bridge was held approximately constant, the ratio of width to normal span varied, as shown in column 4. The originally assumed slab thicknesses are recorded in column 5. The stiffness factors J and H, given in columns 6 and 7, are related by the spacing of the points of the network, since

$$H = \frac{E_1 I_1}{aN}, \qquad J = \frac{\lambda_y^3}{\lambda_x^3} \cdot \frac{E_1 I_1}{\lambda_x N},$$

and therefore

$$J = \frac{\lambda_y^3}{\lambda_x^3} \cdot \frac{a}{\lambda_x} H.$$

The dead loads due to weight of slab (including paving allowance of 25 lb./ft.^{2}) and weight of curb and handrail are given in columns 8 and 9. Live loads were taken as H-20 as specified by the AASHO, so that rear wheel loads, including impact allowances, were as given in column 10. The diameter of the equivalent circular area of loading and the corrective moments given in columns 11 and 12 depend upon the network, as stated in the preceding section. The derivation of these factors is shown in Appendix A. It is sufficient to note here that the corrective moment, when added to the moment found under a wheel load by difference equations, is intended to account for the distribution of the load on a circular area of 1.25 ft. diameter.

Tables 2 and 3 give a summary of the design moments determined for the skew bridges and for the comparative right bridges. Dead load moments are given for all bridges, and live load moments for selected bridges. In addition, comparisons are made between the moments obtained in the skew bridges and in the right bridges. The variations of these moments are discussed in the next section. Influence surfaces and tables of influence ordinates, from which maximum live load moments were obtained, are given in Appendix B.

Because the estimated thickness of slab used in the analyses for the skew bridges did not always coincide with the thickness required by the allowable stresses, some variations in curb details have been made so that the stiffness factors used in the calculations would apply. These variations, shown in Fig. 3, are minor and could be neglected in practice, except for slab 45-C, which has a curb considerably stiffer than the others. Since the heavy curb of slab 45-C was also used in analyzing the comparative right bridge and since the effect of stiffness of curb is similar in skew and right bridges, the comparative moment factors may be said to apply to a bridge having a standard curb.

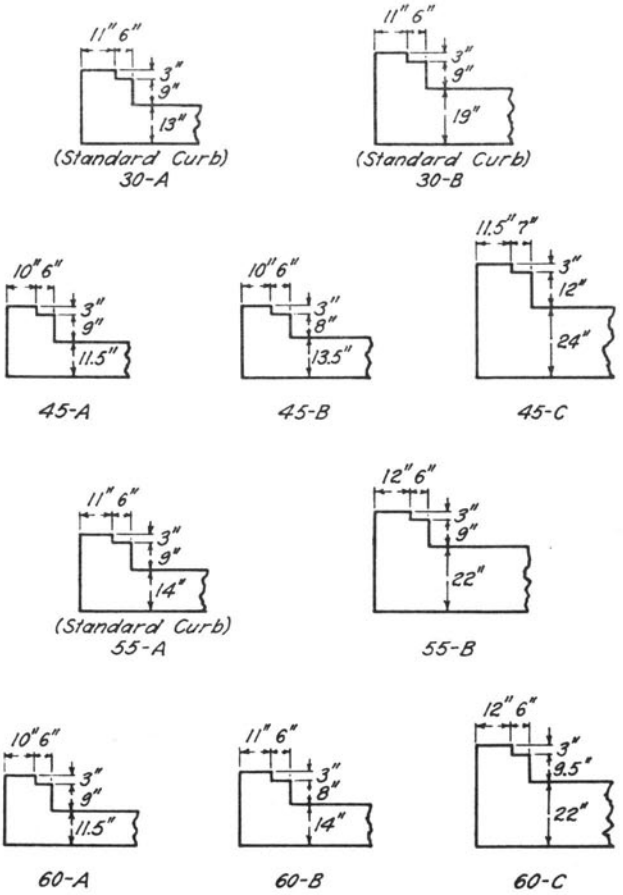

FIG. 3. VARIATION OF CURB DETAIL FROM STANDARD

III. Summary of Live and Dead Load Moments in Skew Slab-Bridges

7. *Presentation of Data.*—Curves showing the dead and live load moments in the curbs and slabs of bridges of different proportions are given in Figs. 4–13. These curves are discussed in detail in the following pages according to the particular moments considered. In judging the numerical results it should be borne in mind that the method of analysis is approximate and that applications may be made only to bridges of a limited range of dimensions. Limitations will be emphasized for the particular moments discussed.

8. *Maximum Dead Load Moment at Center of Slab.*—From the data of columns 2 and 6 of Table 2 the curves of Fig. 4 have been drawn to show the variation of the maximum dead load moment at the center of the slab when the dead load includes the weight of slab, curb, and handrail. For all angles of skew the curves approach a constant value of 0.125 pa^2 at a sufficiently large value of b/a. As the b/a ratio becomes smaller, or in other words as the bridge becomes

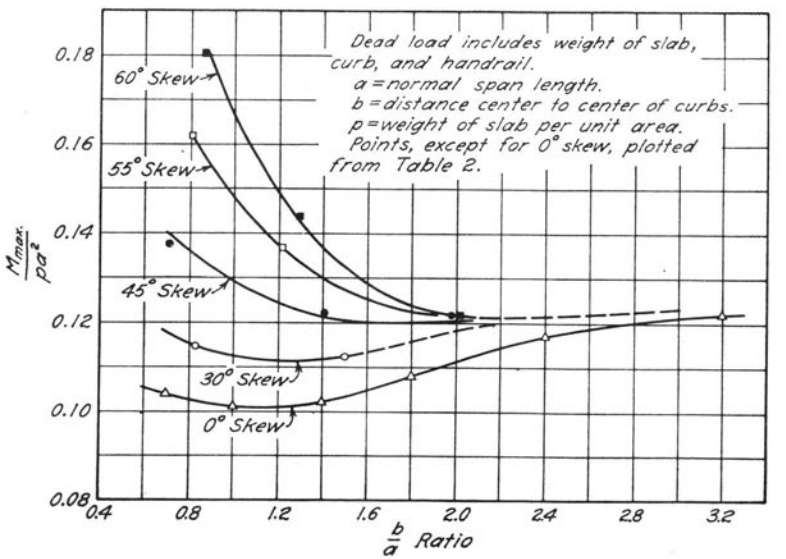

Fig. 4. Maximum Dead Load Moment at Center of Slab, for Skew Bridges with Standard Curb

relatively longer and narrower, the moment coefficient (coefficient of pa^2) in the skew bridge at first decreases and then becomes larger. This increase in moment coefficient at small values of b/a is most marked for the largest angles of skew.

The percentage increase in the maximum dead load moment in skew bridges over the corresponding moment in comparative right bridges is shown in Fig. 5. These curves can be used to obtain the percentage factor for determining the moment in a skew bridge from the corresponding moment in a comparative right bridge.

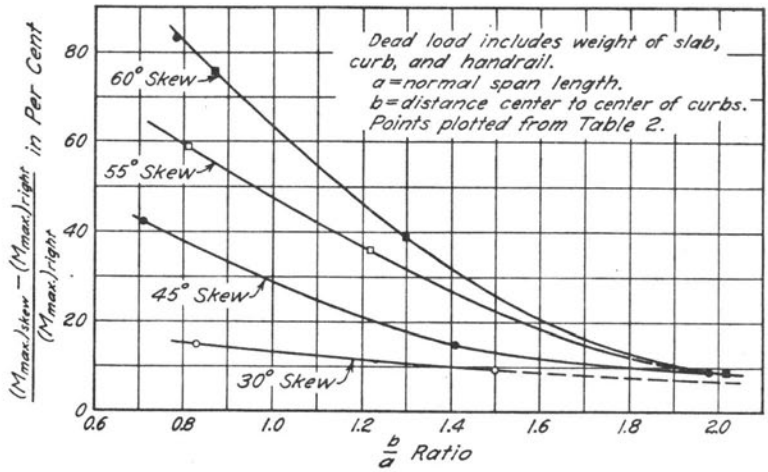

FIG. 5. PERCENTAGE INCREASE IN MAXIMUM DEAD LOAD MOMENT AT CENTER OF SLAB: SKEW-BRIDGE OVER SIMILAR RIGHT BRIDGE, FOR BRIDGES WITH STANDARD CURB

The curves of Figs. 4 and 5 are not limited in their applicability to bridges having a roadway width of 24 ft. They may be used for other roadway widths provided that, for any ratio b/a, the relative stiffness of curb H and the value of q/pa are substantially equal to the values used in the analysis at that ratio of b/a. To aid in determining the values of H and q/pa which are to be used with a given value of b/a, the curves of Fig. 6 have been drawn. As an example of their use, suppose that a slab-bridge is to have a skew of 25 deg., a normal span of 21 ft., and a width, center to center of curbs, of 29.5 ft. The ratio b/a is in this instance $29.5/21 = 1.4$. According to Fig. 6 the

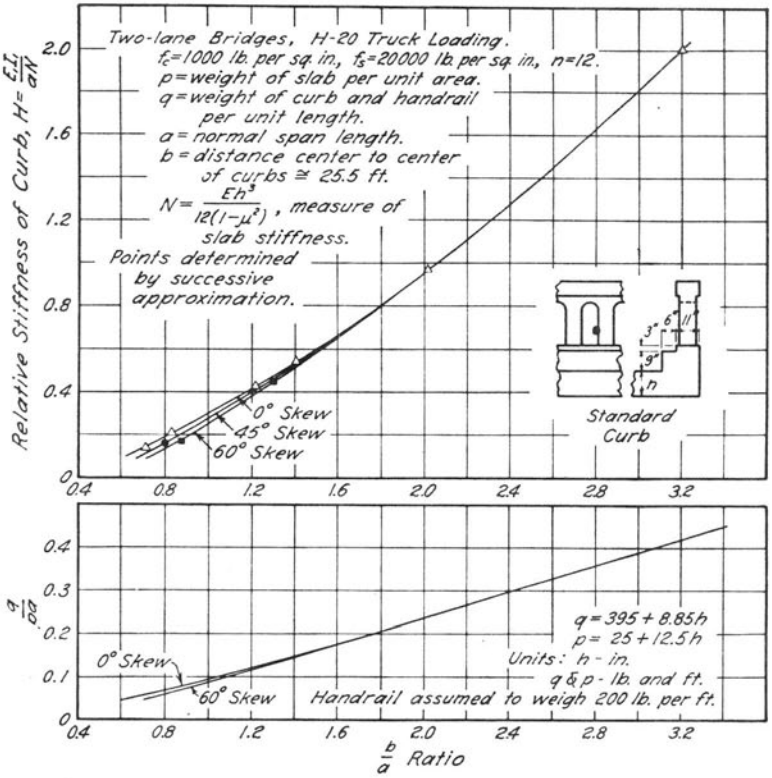

FIG. 6. VARIATION OF H AND q/pa WITH THE b/a RATIO, FOR SKEW BRIDGES WITH STANDARD CURB

values of H and q/pa should be 0.53 and 0.147, respectively, for this bridge in order that the curves of Figs. 4 and 5 may apply. Actually some departure from the values of 0.53 and 0.147 is permissible, since the dead load moment at the center of the bridge varies but little with H and with curb dead load. Furthermore, the variation of moment with H is similar in the right and skew bridges, so that the percentage factors given in Fig. 5 remain valid with reasonable accuracy.

The direction of maximum dead load moment at the center of the skew bridge tends to become normal to the abutments as the b/a ratio increases, finally becoming and remaining normal to the abutments. This is shown by the angles given in Table 2 and by the curves

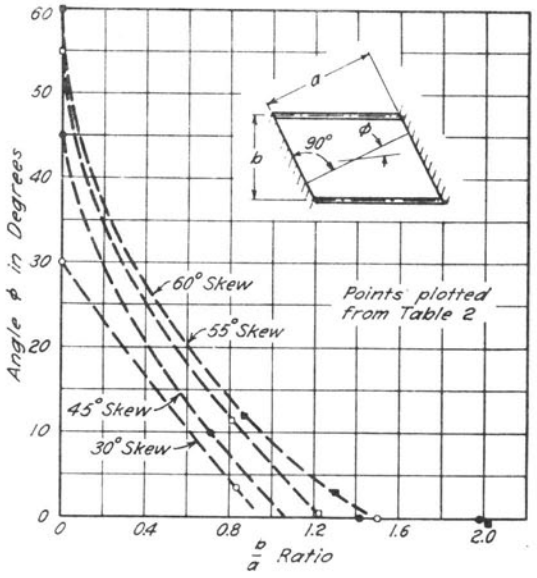

FIG. 7. DIRECTION OF MAXIMUM DEAD LOAD MOMENT AT CENTER OF SLAB, FOR SKEW BRIDGES WITH STANDARD CURB

of Fig. 7, which give, for each angle of skew, the angle of departure from a line drawn normal to the abutments. The significant feature is that the direction of maximum dead load moment departs from the direction of the normal span by only small angles for all the slabs analyzed. The maximum departure is about 14 degrees for a slab of 60-deg. skew having a b/a ratio of 0.8.

A feature of dead load moments in skew slabs is that, for the larger ratios of b/a, maximum dead load moments occur at points near the blunt corner of the slab. However, it seems unlikely that, when truck loadings are considered, these points would have greater total moments due to dead load plus live load. An investigation of this possibility for slab 60-B showed that, whereas the maximum dead load moment at point 7 is 8.7 per cent greater than at point 11, the maximum moment due to dead and live loads combined is about 7.3 per cent less at point 7 than at point 11.

Another feature which distinguishes the action of skew slabs from that of right slabs is the rather large negative moment produced in

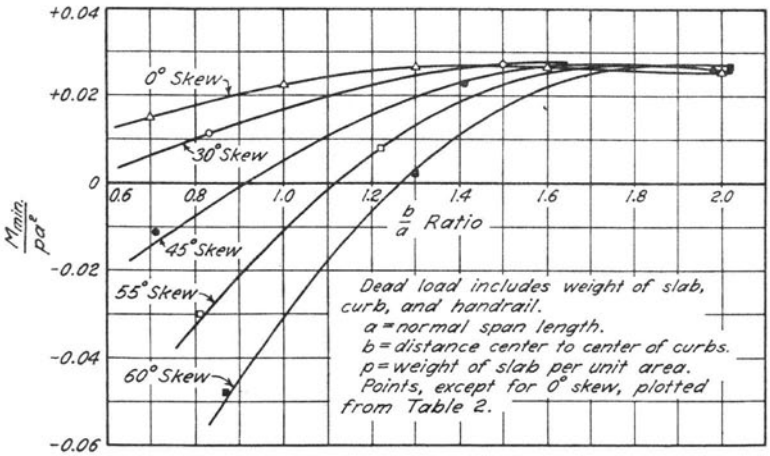

FIG. 8. MINIMUM DEAD LOAD MOMENT AT CENTER OF SLAB, FOR SKEW BRIDGES WITH STANDARD CURB

the neighborhood of the blunt corner. For three of the slab bridges, maximum negative live load moments at points near the blunt corners are given in Table 3, column 8. These moments occur for wheel loads placed at some distance away from the point under consideration. They act on a section of the slab which lies parallel to a line roughly bisecting the angle at the blunt corner. It is observed that the magnitudes of these moments increase with both span length and angle of skew.

9. *Minimum Dead Load Moment at Center of Slab.*—Values of dead load moment in a direction at right angles to the maximum moment, for bridges of various skew, are shown in Fig. 8. It may be observed that this minimum dead load moment at the centers of the bridges becomes negative for the smaller ratios of b/a and for the larger angles of skew. In particular, for slab 60-C the negative dead load moment, when combined with additional negative live load moment, requires that the top steel parallel to the supports be about 25 per cent as much as the bottom steel normal to the supports.

The same limitations apply to the use of the curves of minimum dead load moment as apply to the use of the curves of maximum dead load moment. These are discussed in the preceding paragraphs.

10. *Maximum Live Load Moment at Center of Slab.*—Live load moments were determined for a number of bridges for H-20 truck loading. The moments reported herein are based on an assumption that the two lanes of traffic always head in opposite directions and remain on the right-hand side of the roadway. Furthermore, opposite hand skews are not considered. By reversal of the directions of traffic, moments may readily be determined from the influence surfaces for angles of skew opposite in sign to those used herein. Numerical values of moments applying to traffic lanes heading in the same direction or to opposite-hand skews were not computed by the authors, and are consequently not reported here. In general, the difference in maximum live load moments for these conditions would not be important.

A comparison of the maximum live load moment at the center of the slabs of skew and right bridges gave the percentage factors indicated in column 5 of Table 3 and in Fig. 9. These factors give the percentage increase in moment in the skew bridges over that in the comparative right bridges.

The dashed portions of the curves in Fig. 9 show the variation in the percentage factor for small spans when only the inner rear truck wheels in each lane are on the bridge. When the spans are larger, however, one or more outer rear truck wheels are required on the

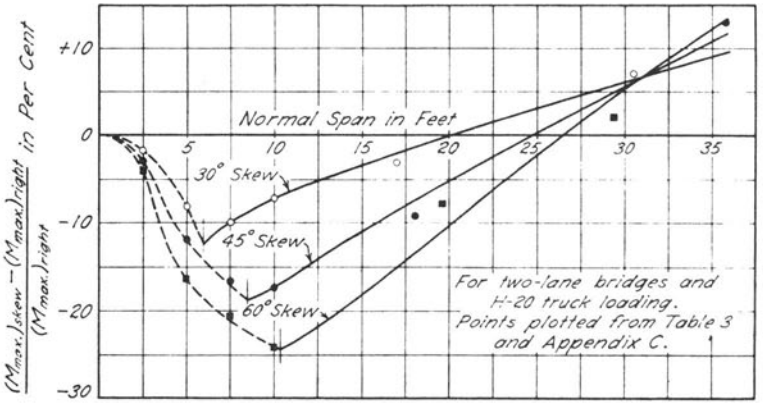

FIG. 9. PERCENTAGE INCREASE IN MAXIMUM LIVE LOAD MOMENT AT CENTER OF SLAB: SKEW BRIDGE OVER SIMILAR RIGHT BRIDGE, FOR BRIDGES WITH STANDARD CURB

bridge in order to produce maximum moment. The procedure for obtaining the moment in the slabs of short span is described in Appendix C.

The percentage factor for the larger spans is shown by the solid portions of the curves of Fig. 9. At the span lengths for which a truck wheel is over an abutment for maximum moment at the center of the slab the trends of the curves of Fig. 9 change. Only one such change in trend (cusp) for each curve is shown. This is the effect of the outer wheel of Truck No. 1 (see Appendix C). A cusp in each curve occurs also for Truck No. 2, though it is not shown in Fig. 9. It occurs for larger spans than the first cusp and is not as pronounced. Its exact location and nature are difficult to determine, since influence surfaces for a sufficient number of spans in its range are not available. The effect was calculated approximately by the use of an influence surface for the infinite strip slab, and upon such a basis the solid portions of the curves of Fig. 9 were sketched in.

It is significant that the percentage factors are positive for the larger spans only and that these factors are small. For the shorter spans the percentage factors are negative, indicating that the maximum live load moment at the center of the skew spans is less than the corresponding moment in comparative right bridges. The decrease becomes more marked as the angle of skew becomes larger.

Because of the definite spacing of the wheel loads, the calculated live load moments apply only to bridges having a clear roadway of about 24 ft. and having normal spans as indicated in Fig. 1. For other widths of roadway the influence surfaces given in Appendix B may be applied, provided that the ratio of sides is maintained, the relative stiffness of curb H is maintained (see Fig. 6), and the corrective moments under the load (see Equation [6] and Appendix A) are modified.

A comparison of columns 8 and 6 of Tables 2 and 3, respectively, shows that the directions of maximum dead load moment and maximum live load moment do not differ greatly at the center of the slab, the greatest angle between them being about 4½ deg. for the slabs analyzed.

11. *Secondary Live Load Moment at Center of Slab.*—For live load moment at the center of the slab in a direction parallel to the supports, the influence surfaces show that either positive or negative moment is possible, depending upon the positions of the loads. The negative moment becomes important only for the larger angles of skew and the larger spans.

The positive live load moment in a direction perpendicular to the direction of maximum live load moment, produced by the same position of wheel loads that causes the maximum moment, is shown in column 7 of Table 3. The ratio of this positive minimum live load moment to the maximum live load moment is shown in Fig. 10; it varies generally between 30 and 70 per cent. For combined live and dead loads, however, the ratios of lateral to spanwise moments become considerably reduced.

12. *Maximum Dead Load Moment in Curb.*—The maximum moment in the curb is more sensitive than the moment at the center of the slab to variations in relative stiffness and weight of the curb. Whether the curb be on a skew or right bridge, the increase of relative stiffness of the curb has a pronounced effect in increasing the moment resisted by the curb. Because the curbs varied somewhat from the adopted standard detail, the actual moments found in the curbs of the skew bridges, given by column 4 of Table 2 and plotted in Fig. 11, are considered to be subject to greater error than the moments computed for the slab center. The moments shown by the curves in Fig. 11 were adjusted to values which seem reasonable for standard curbs. The percentages plotted in Fig. 12 from column 5 of Table 2 indicate the increase in maximum dead load moment in the curbs of skew bridges over the corresponding moment in the curbs of right bridges of identical normal span, width, and curb detail.

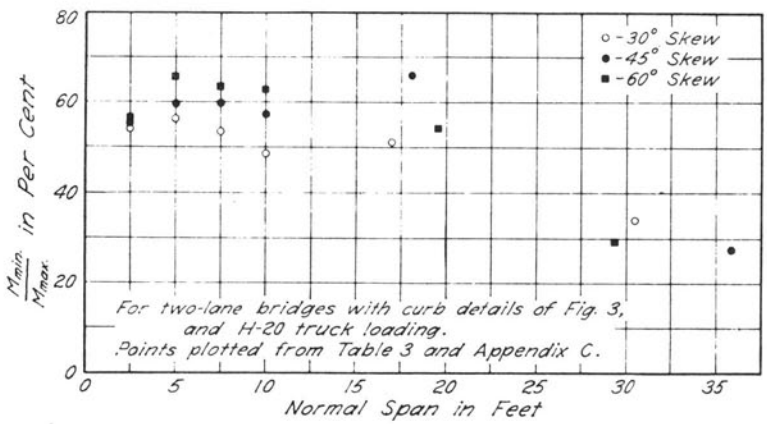

FIG. 10. RATIO OF MINIMUM TO MAXIMUM LIVE LOAD MOMENT AT CENTER OF SLAB, FOR LOADS PLACED TO PRODUCE MAXIMUM LIVE LOAD MOMENT

They may be said to apply with reasonable accuracy to bridges having standard curb detail.

The angle of skew has practically no effect on the coefficient of dead load moment in the curbs of bridges having a b/a ratio of about 0.8 or less. The effect of angle of skew becomes increasingly marked as the ratio b/a becomes larger. When b/a is 2.0 the maximum dead load moment in the curb of a bridge of 60-deg. skew is 66 per cent greater than that in the curb of a comparative right bridge.

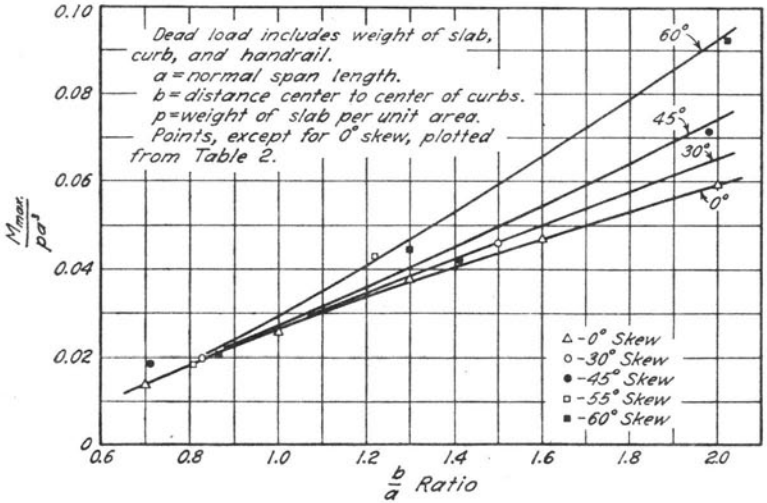

FIG. 11. MAXIMUM DEAD LOAD MOMENT IN CURB, FOR SKEW BRIDGES WITH STANDARD CURB

In general, the same limitations apply to the use of the curves of dead load moment in the curb as apply to the use of curves of other dead load moments discussed previously. However, if the percentages given in Fig. 12 are applied to bridges having relative curb stiffnesses and weights other than those used in the analyses and defined in Fig. 6, an appreciable error may be introduced into the curb moments. Further calculations are needed to determine the possible magnitudes of such errors; and unless these calculations are made, the given percentages must be applied with caution to bridges having relative curb stiffnesses other than those used in the analyses.

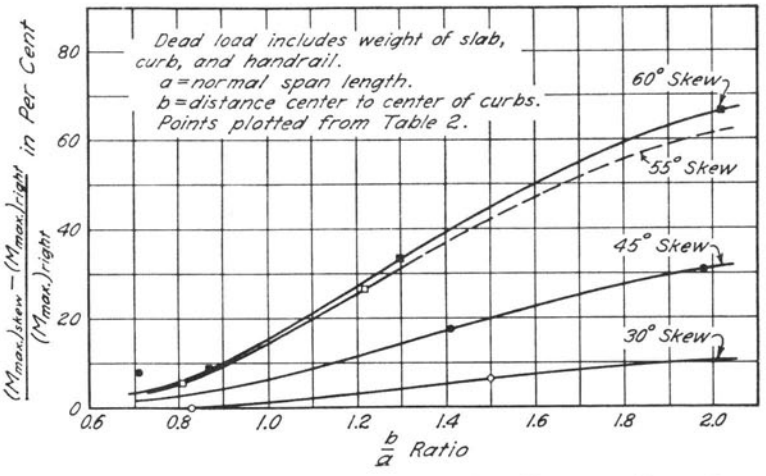

FIG. 12. PERCENTAGE INCREASE IN MAXIMUM DEAD LOAD MOMENT IN CURB: SKEW BRIDGE OVER SIMILAR RIGHT BRIDGE, FOR BRIDGES WITH STANDARD CURB

13. *Maximum Live Load Moment in Curb.*—The calculated live load moments in the curbs are subject to errors due to limitations of the method of calculation employed. It is recognized that the maximum moment determined at a point on the network might be increased if a different network were used. Furthermore, the live load moment in the curb is considerably affected by variations in the relative stiffness of the curb. While an attempt was made to use a parabolic interpolation in order to correct for the spacing of points in the network, irregularities remain in the trend of the results. The maximum live load moments corresponding to the curbs shown in Fig. 3 are given by column 2 of Table 3 and are plotted in Fig. 13.

The most significant result which can be determined from Table 2 is that the difference in live load moment in the curbs of skew bridges is within a range of about plus to minus 10 per cent of the moment in the curbs of the comparative right bridges.

Again, the calculated live load moments apply only to bridges having a clear roadway of about 24 ft. and normal spans as indicated in Fig. 1. For other widths of roadway the influence surfaces of Appendix B may be applied, provided that the ratio of sides and the relative stiffness of curb are maintained (see Fig. 6).

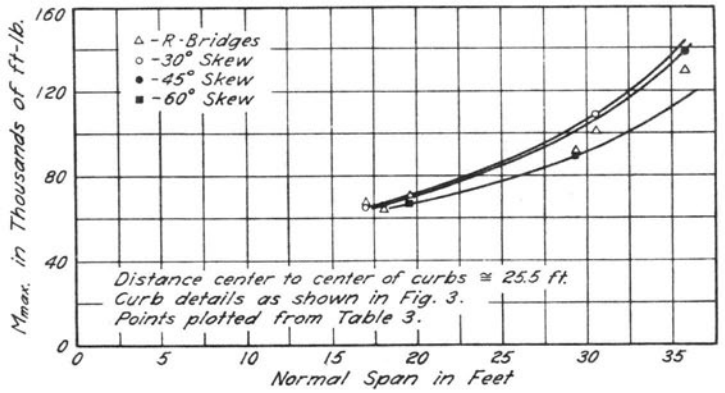

FIG. 13. MAXIMUM LIVE LOAD MOMENT IN CURB, FOR TWO-LANE SKEW BRIDGES WITH H-20 TRUCK LOADING

IV. Summary

The results of this investigation of moments in skew slab-bridges have been derived by a method which may be stated as follows:

1. The dimensions of a skew bridge are selected to suit a convenient network of intersecting lines.

2. Standard curb dimensions are adopted, and the required slab thickness of the skew bridge is estimated.

3. The skew bridge is analyzed by means of difference equations. Influence surfaces are constructed in order to determine live load effects. Dead load effects are determined from the influence surfaces or by a direct difference equation solution.

4. The required slab thickness is calculated according to the moments given by the analysis, the allowable stresses being taken into account. When the required slab thickness differs from the estimated slab thickness, an adjustment in the curb dimensions is made in order to maintain the curb and slab stiffnesses in the same ratio as used in the analysis.

5. Analyses of a series of bridges of varying span length and angle of skew yield data which are reported in tables and curves showing the effects of the bridge parameters on maximum and minimum live and dead load moments.

6. Moments in right bridges, which are designated as comparative right bridges, are calculated. From these moments and those in the skew bridges, factors which give a percentage increase in maximum moments in the skew bridges over the maximum moments in the comparative right bridges are computed, and reported in tables and curves. A comparative right bridge is one which has span length, width of roadway, curb and handrail detail, and slab thickness identical to those dimensions in the skew bridge, span length in both cases being measured normal to the supports.

7. Dead and live load effects are reported separately. The live load moment curves are valid only for bridges accommodating two lanes of H-20 truck traffic, with curbs at a distance apart of about 25.5 ft. The dead load moment curves are applicable to bridges of any width-span ratio. However, there are other limitations in the use of both the dead and live load moment curves. These are emphasized in the text.

From a study of the results of analyses of bridges within the range considered in this bulletin, the following observations are made:

1. The curves of Figs. 4–13 may be used for the design of skew slab-bridges with curbs, if the limiting range of application of the curves is understood and not exceeded.

2. The curves of Fig. 6 emphasize the fact that the results given in this bulletin are for bridges in which the curb and handrail details do not vary appreciably. These curves may be of value in estimating the required slab thickness preparatory to an analysis of a skew bridge.

3. The maximum dead load moment coefficient at the center of the slab, shown in Fig. 4, approaches that for a simple beam (namely 0.125) for small spans (large values of b/a). As the b/a ratio becomes smaller the moment coefficient at first decreases and then becomes larger, the increase being most marked for the largest angles of skew. All the curves of Fig. 4 represent conditions for bridges in which the slabs are designed for given working stresses and the curbs are of a constant dimension.

4. The minimum dead load moment coefficient at the center of the slab, shown in Fig. 8, approaches a value equal to Poisson's ratio times 0.125 at large values of b/a. As the b/a ratio becomes smaller the moment coefficient at first increases slightly in the positive range, and then becomes smaller, the decrease carrying the coefficients for the largest angles of skew into the negative range.

5. The maximum live load moment at the center of the slab in the skew bridge (see Fig. 9) is less than in the comparative right bridge when normal spans are less than 20 ft. and angles of skew are 30 deg. or greater.

6. The secondary live load moment at center of the slab in the skew bridge (see Fig. 10) is positive; it ranges from about 30 to 70 per cent of the maximum live load moment. In general the percentage is higher for the larger angles of skew.

7. The maximum dead load moment coefficient in a curb, shown in Fig. 11, increases with decreasing span (increasing values of b/a). For the smaller spans the moment coefficient increases with angle of skew, but for larger spans the coefficient approaches a value independent of angle of skew. All the curves of Fig. 11 represent conditions for bridges in which the curbs are of a constant dimension.

8. The maximum live load moment in a curb, shown in Fig. 13, is within a range of plus or minus 10 per cent of the corresponding moment in the comparative right bridge. This moment increases with increasing angle of skew.

9. The maximum live and dead load moments in a curb are quite sensitive to the relative curb-slab stiffness. They occur at points between the center of the curb span and the blunt corner of the bridge.

10. The direction of maximum moment at the center of the slab is inclined only slightly away from the normal span direction toward the skew span direction.

APPENDIX A

Study of Effective Loaded Areas for Rectangular and Triangular Networks in Difference Equation Solutions

In order to determine the effective concentration of a load at one point on a difference equation network for rectangular and triangular nets, analyses of two simply supported rectangular plates carrying a central load were made by means of difference equations as well as by means of the differential equation solution with the formulas and numerical constants given in Bulletin 315.[7]

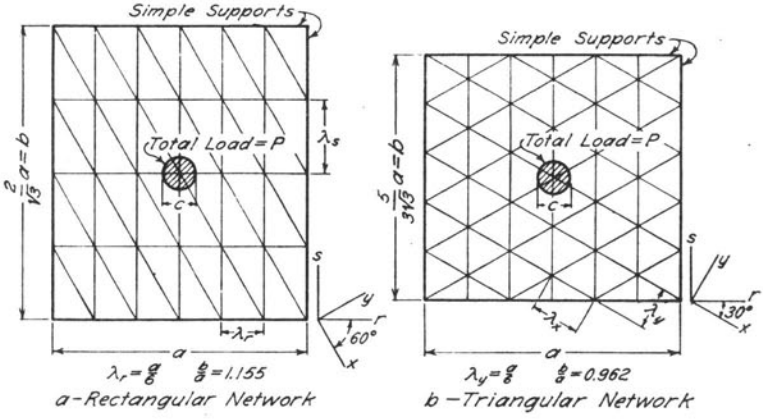

Fig. 14. Rectangular and Triangular Networks Investigated for Effective Loaded Area

In the case of the network used for the 60-deg. skew bridges, the networks may be considered rectangular, of the form shown in Fig. 14a. From the solution by difference equations, the moments under the load P are

$$M_r = 0.264P$$

$$M_s = 0.233P.$$

From the solution by differential equations (Bulletin 315), the moment M_r is

$$M_r = M_{or} - 0.034P. \qquad (7)$$

[7] V. P. Jensen, "Moments in Simple Span Bridge Slabs with Stiffened Edges," Univ. of Ill. Eng. Exp. Sta. Bul. 315, 1939.

Westergaard's approximate value of M_{or} is

$$M_{or} = \frac{P}{2.32 + \frac{8c_r}{a}}$$

and, from Equation (7),

$$M_{or} = 0.034P + M_r = 0.034P + 0.264P = 0.298P.$$

Since the two values of M_{or} are to be equal, the value of c_r/a is determined as

$$c_r/a = 0.130.$$

With $a = 6\lambda_r$, one obtains the result

$$c_r = 0.78\lambda_r.$$

From the differential equation solution (Bulletin 315), M_s is

$$M_s = M_{os} + 0.015P. \tag{8}$$

Westergaard's approximate value of M_{os} is

$$M_{os} = \frac{P}{2.32 + 8\frac{c_s}{a}} - 0.068P$$

and, from Equation (8),

$$M_{os} = -0.015P + M_s = -0.015P + 0.233P = 0.218P.$$

Since the two values of M_{os} are to be equal, the value of c_s/a is determined as

$$c_s/a = 0.147,$$

whence

$$c_s = 0.88\lambda_r = 0.51\lambda_s.$$

These values of c are those which must be assumed to apply if no corrections are made to the influence ordinates at the point under the load, as determined by difference equations.

For the 30-deg. skew bridges the networks are triangular, of the form shown in Fig. 14b. In a manner similar to that employed for the

rectangular network, the value of c is calculated as follows. From the difference equation solution,

$$M_r = 0.267P$$

$$M_s = 0.274P.$$

The differential equation solution for M_r is

$$M_r = M_{or} - 0.053P.$$

Further, $M_{or} = \dfrac{P}{2.32 + 8\dfrac{c}{a}} = 0.053P + 0.267P = 0.320P,$

from which

$$c/a = 0.100$$

and, with $a = 6\lambda_y$, one obtains the result

$$c = 0.60\lambda_y.$$

The differential equations give also

$$M_s = M_{os} + 0.019P.$$

With

$$M_{os} = \frac{P}{2.32 + 8\dfrac{c}{a}} - 0.068P = -0.019P + 0.274P,$$

the value of c/a becomes

$$c/a = 0.097,$$

or

$$c = 0.58\lambda_y.$$

The average value of c is

$$c = 0.59\lambda_y,$$

valid for both the r and s directions.

APPENDIX B

Tables of Influence Ordinates and Diagrams of Influence Surfaces for Moments in Slabs and Curbs

Table 4

Ordinates of Influence Surfaces for Moments in Slab 30-A

Data: 30-deg. skew; $b/a = 1.50$; $H = 0.58$; $\mu = 0.2$

The ordinates were computed for the sections at point 11 in the slab and at point 2 in the curb, as shown in Fig. 1. Contour lines on the influence surfaces are shown in Fig. 15.

Influence Ordinates

Pt.	M_x, pt. 11	M_y, pt. 11	M_{xy}, pt. 11	M_{curb}, pt. 2
1	0.0125	−0.0045	+0.0145	0.0685 a
2	0.0219	−0.0067	+0.0230	0.1588 a
3	0.0221	+0.0033	+0.0210	0.0626 a
4	0.0199	−0.0051	+0.0176	0.0668 a
5	0.0510	+0.0086	+0.0369	0.0719 a
6	0.0393	+0.0270	+0.0305	0.0336 a
7	0.0555	+0.0095	+0.0205	0.0321 a
8	0.1138	+0.0504	+0.0552	0.0331 a
9	0.0545	+0.0917	+0.0211	0.0160 a
10	0.1003	+0.0457	−0.0055	0.0153 a
11	0.2650 0.322*	+0.2340 +0.291*	+0.0271	0.0152 a
10′				0.0073 a
9′				0.0071 a
8′				0.0069 a
7′				0.0032 a
6′	Ordinates same as for corresponding symmetrical points			0.0032 a
5′				0.0030 a
4′				0.0009 a
3′				0.0014 a
2′				0.0010 a
1′				0.0006 a
	Totals for Dead Load with $q/pa = 0.1510$			
	0.0910 pa^2	0.0485 pa^2	0.0367 pa^2	0.0462 pa^2

* Corrected for wheel load on 1.25-ft. diam. circular area on a slab of 17.00-ft. span.

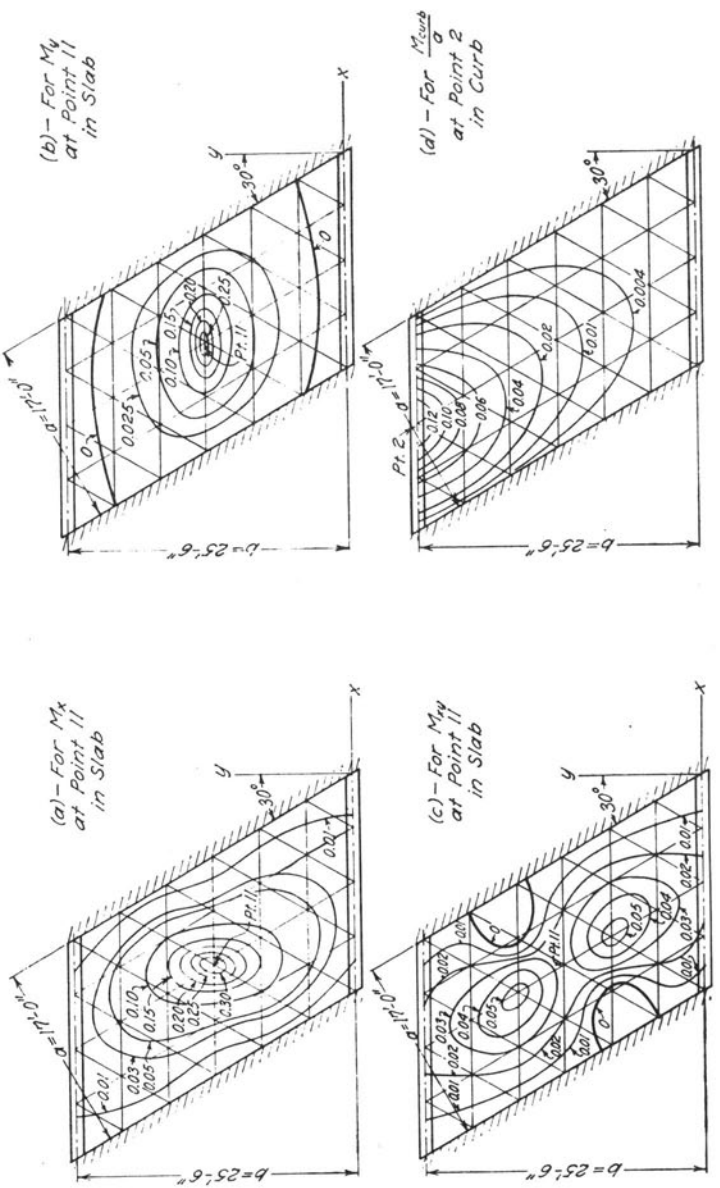

FIG. 15. INFLUENCE SURFACES FOR MOMENTS IN SLAB 30-A

TABLE 5

ORDINATES OF INFLUENCE SURFACES FOR MOMENTS IN SLAB 30-B

Data: 30-deg. skew; $b/a = 0.83$; $H = 0.194$; $\mu = 0.2$

The ordinates were computed for the sections at point 13 in the slab and at points 4 and 7 in the curb, as shown in Fig. 1. Contour lines on the influence surfaces are shown in Fig. 16.

Influence Ordinates

Pt.	M_x, pt. 13	M_y, pt. 13	M_{xy}, pt. 15	M_{curb}, pt. 4	M_{curb}, pt. 7
1	0.0459	−0.0114	0.0445	0.0213 a	0.0110 a
2	0.0925	−0.0198	0.0794	0.0481 a	0.0245 a
3	0.0470	+0.0098	0.0399	0.0229 a	0.0126 a
4	0.1352	−0.0278	0.0909	0.0927 a	0.0450 a
5	0.1027	+0.0349	0.0702	0.0477 a	0.0281 a
6	0.0490	+0.0432	0.0286	0.0204 a	0.0135 a
7	0.1419	−0.0280	0.0597	0.0470 a	0.0841 a
8	0.1878	+0.0540	0.0870	0.0497 a	0.0469 a
9	0.1175	+0.1212	0.0439	0.0318 a	0.0268 a
10	0.0656	+0.0466	0.0101	0.0141 a	0.0121 a
11	0.0866	−0.0135	0.0185	0.0200 a	0.0330 a
12	0.1754	+0.0579	0.0158	0.0293 a	0.0438 a
13	0.3319 0.387*	+0.2590 +0.314*	0.0477	0.0288 a	0.0328 a
14	0.1676	+0.0731	0.0098	0.0197 a	0.0204 a
15	0.0743	+0.0184	0.0096	0.0089 a	0.0093 a
15′	0.0681	+0.0413	0.0119	0.0124 a	0.0193 a
14′	0.1145	+0.1257	0.0413	0.0181 a	0.0255 a
13′	0.1758	+0.0751	0.0774	0.0173 a	0.0216 a
12′	0.1220	+0.0199	0.0431	0.0119 a	0.0143 a
11′	0.0565	−0.0086	0.0271	0.0048 a	0.0062 a
10′	0.0453	+0.0486	0.0254	0.0079 a	0.0118 a
9′	0.0899	+0.0549	0.0590	0.0113 a	0.0158 a
8′	0.1097	+0.0188	0.0688	0.0106 a	0.0142 a
7′	0.0837	−0.0147	0.0549	0.0069 a	0.0096 a
6′	0.0381	+0.0221	0.0286	0.0051 a	0.0074 a
5′	0.0687	+0.0127	0.0568	0.0072 a	0.0103 a
4′	0.0785	−0.0143	0.0658	0.0066 a	0.0097 a
3′	0.0320	+0.0032	0.0308	0.0033 a	0.0050 a
2′	0.0559	−0.0110	0.0547	0.0048 a	0.0073 a
1′	0.0282	−0.0065	0.0300	0.0024 a	0.0038 a
	Totals for Dead Load with $q/pa = 0.0708$				
	0.0940 pa^2	0.0320 pa^2	0.0415 pa^2	0.0197 pa^2	0.0195 pa^2

* Corrected for wheel load on 1.25-ft. diam. circular area on a slab of 30.5-ft. span.

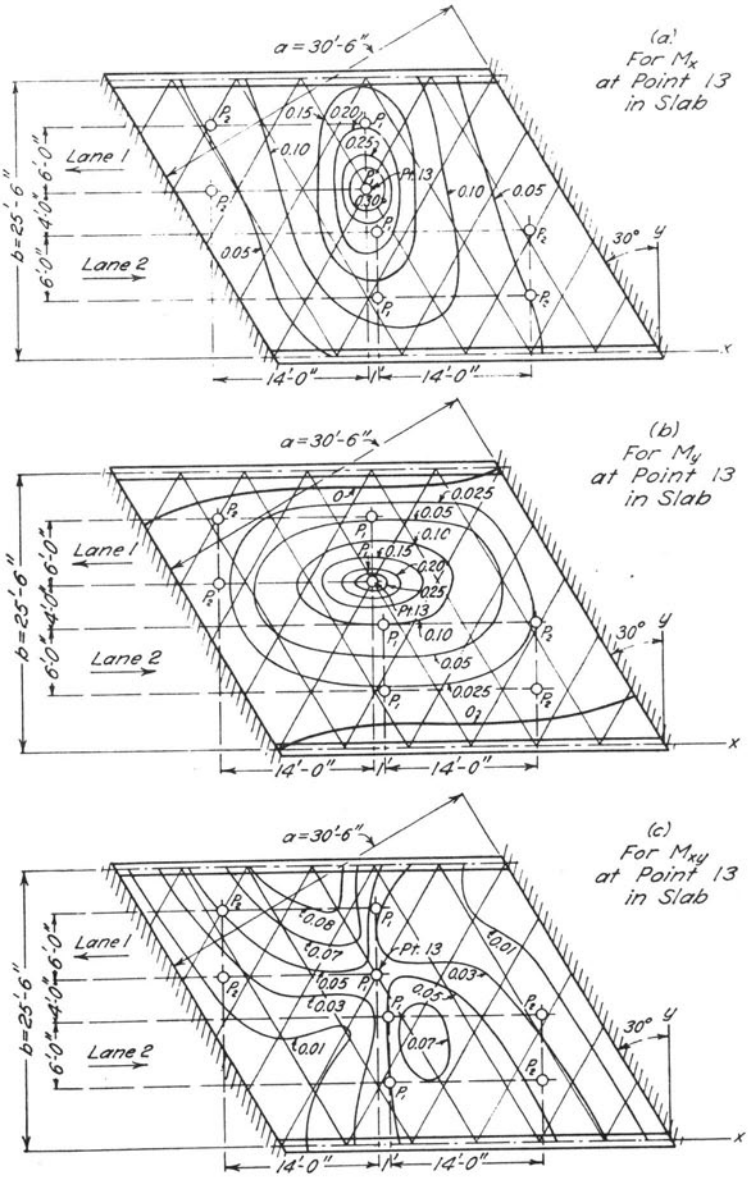

FIG. 16. INFLUENCE SURFACES FOR MOMENTS IN SLAB 30-B

Parts (a) – (c). The figure concludes on page 48.

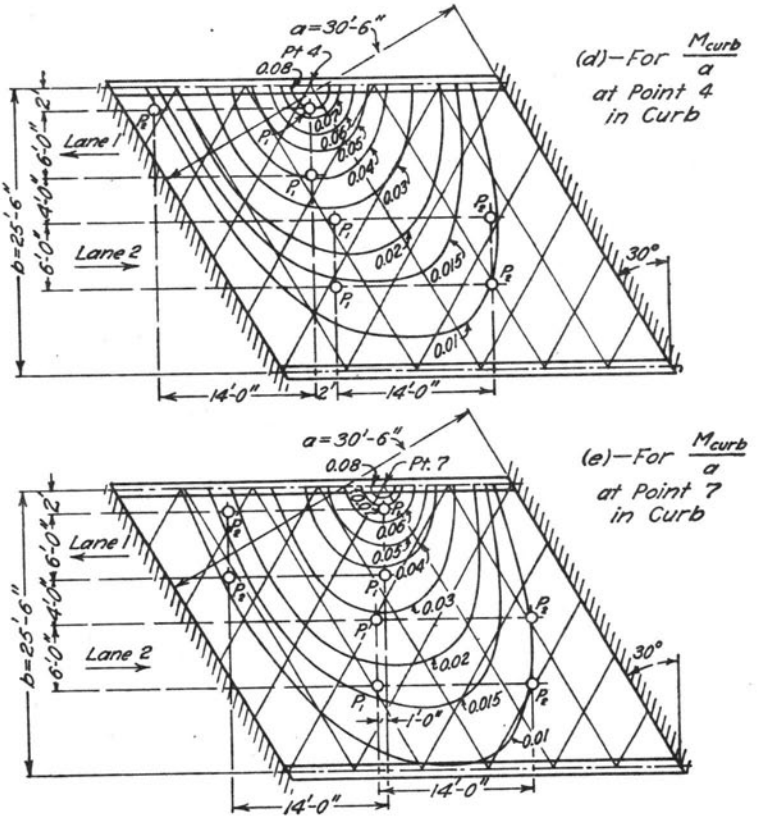

FIG. 16. INFLUENCE SURFACES FOR MOMENTS IN SLAB 30-B
Parts (d) and (e).

TABLE 6

ORDINATES OF INFLUENCE SURFACES FOR MOMENTS IN SLAB 45-B

Data: 45-deg. skew; $b/a = 1.41$; $H = 0.424$; $\mu = 0.2$

The ordinates were computed for the sections at point 12 in the slab and at point 4 in the curb, as shown in Fig. 1. Contour lines on the influence surfaces are shown in Fig. 17.

Influence Ordinates

Pt.	M_r, pt. 12	M_s, pt. 12	M_{curb}, pt. 4
1	0.0206	−0.0169	0.0291 a
2	0.0394	−0.0298	0.0684 a
3	0.0275	−0.0133	0.0346 a
4	0.0502	−0.0334	0.1343 a
5	0.0622	−0.0156	0.0667 a
6	0.0473	+0.0085	0.0245 a
7	0.0416	−0.0226	0.0527 a
8	0.0970	−0.0006	0.0396 a
9	0.1166	+0.0584	0.0219 a
10	0.0474	+0.0405	0.0074 a
11	0.0950	+0.0440	0.0132 a
12	0.2600 0.352*	+0.1976 +0.290*	0.0118 a
12′	0.1155	+0.0599	0.0065 a
11′	0.0457	+0.0104	0.0022 a
10′	0.0942	+0.0451	0.0040 a
9′	0.0942	+0.0045	0.0035 a
8′	0.0569	−0.0089	0.0019 a
7′	0.0214	−0.0118	0.0005 a
6′	0.0386	−0.0077	0.0012 a
5′	0.0383	−0.0142	0.0010 a
4′	0.0262	−0.0175	0.0005 a
3′	0.0158	−0.0085	0.0003 a
2′	0.0203	−0.0153	0.0003 a
1′	0.0105	−0.0085	0.0001 a
	Totals for Dead Load with $q/pa = 0.1416$		
	0.1186 pa^2	0.0196 pa^2	0.0421 pa^2

* Corrected for wheel load on 1.25-ft. diam. circular area on a slab of 18.04-ft. span.

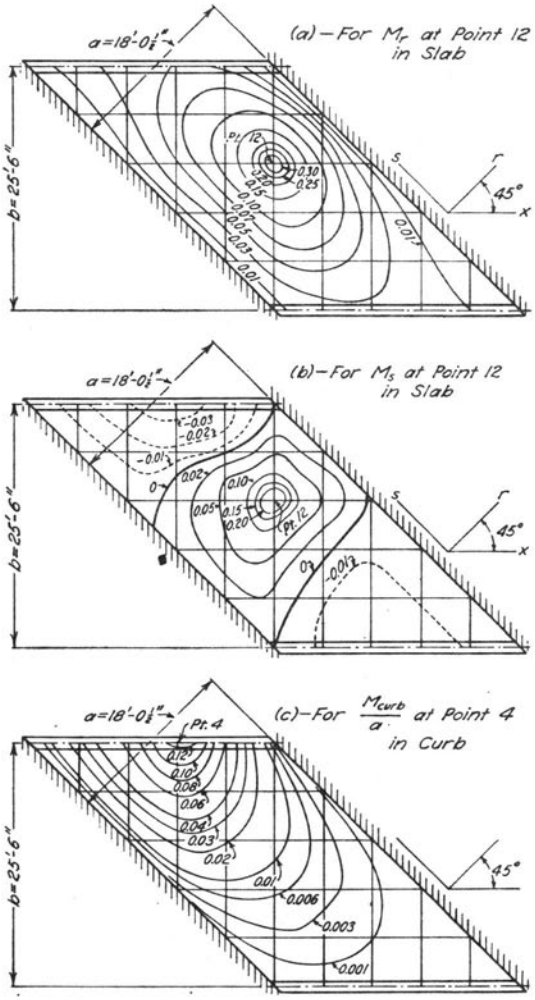

FIG. 17. INFLUENCE SURFACES FOR MOMENTS IN SLAB 45-B

TABLE 7

ORDINATES OF INFLUENCE SURFACES FOR MOMENTS IN SLAB 45-C

Data: 45-deg. skew; $b/a = 0.71$; $H = 0.177$; $\mu = 0.2$

The ordinates were computed for the sections at point 18 in the slab and at points 7 and 11 in the curb, as shown on Fig. 1. Contour lines on the influence surfaces are shown in Fig. 18.

Influence Ordinates

Pt.	M_x, pt. 18	M_y, pt. 18	M_{xy}, pt. 18	M_{curb}, pt. 7	M_{curb}, pt. 11
1	0.0186	−0.0041	0.0398	0.0130 a	0.0073 a
2	0.0383	−0.0063	0.0770	0.0286 a	0.0161 a
3	0.0201	+0.0029	0.0381	0.0153 a	0.0089 a
4	0.0609	−0.0064	0.1070	0.0507 a	0.0283 a
5	0.0442	+0.0168	0.0712	0.0334 a	0.0206 a
6	0.0235	+0.0246	0.0329	0.0155 a	0.0108 a
7	0.0876	−0.0069	0.1234	0.0884 a	0.0476 a
8	0.0783	+0.0391	0.0956	0.0508 a	0.0355 a
9	0.0592	+0.0704	0.0562	0.0266 a	0.0222 a
10	0.0403	+0.0364	0.0202	0.0103 a	0.0100 a
11	0.1146	−0.0109	0.1170	0.0495 a	0.0828 a
12	0.1307	+0.0619	0.1060	0.0371 a	0.0501 a
13	0.1272	+0.1426	0.0699	0.0239 a	0.0301 a
14	0.1094	+0.0632	0.0362	0.0126 a	0.0165 a
15	0.0679	−0.0039	0.0319	0.0109 a	0.0168 a
16	0.1229	−0.0156	0.0787	0.0264 a	0.0417 a
17	0.1983	+0.0679	0.0755	0.0227 a	0.0342 a
18	0.3142 0.394*	+0.2579 +0.339*	0.0744	0.0169 a	0.0250 a
17′				0.0106 a	0.0163 a
16′				0.0045 a	0.0087 a
15′				0.0037 a	0.0061 a
14′				0.0116 a	0.0183 a
13′				0.0101 a	0.0165 a
12′				0.0073 a	0.0128 a
11′				0.0038 a	0.0087 a
10′	Ordinates same as for corresponding symmetrical points			0.0041 a	0.0068 a
9′				0.0050 a	0.0089 a
8′				0.0042 a	0.0086 a
7′				0.0027 a	0.0072 a
6′				0.0017 a	0.0035 a
5′				0.0021 a	0.0049 a
4′				0.0016 a	0.0052 a
3′				0.0007 a	0.0020 a
2′				0.0008 a	0.0033 a
1′				0.0003 a	0.0016 a
	Totals for Dead Load with $q/pa = 0.0599$				
	0.0884 pa^2	0.0380 pa^2	0.0700 pa^2	0.0175 pa^2	0.0186 pa^2

* Corrected for wheel load on 1.25-ft. diam. circular area on slab of 35.8-ft. span.

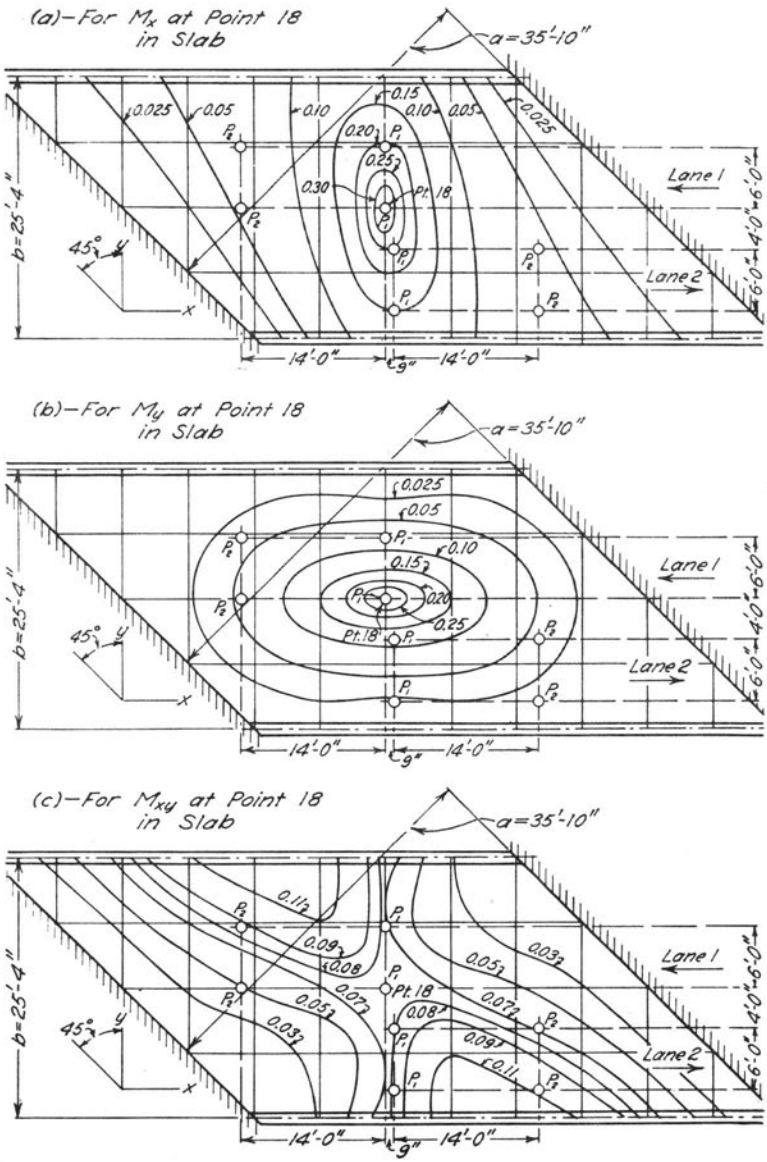

FIG. 18. INFLUENCE SURFACES FOR MOMENTS IN SLAB 45-C
Parts (a) – (c).

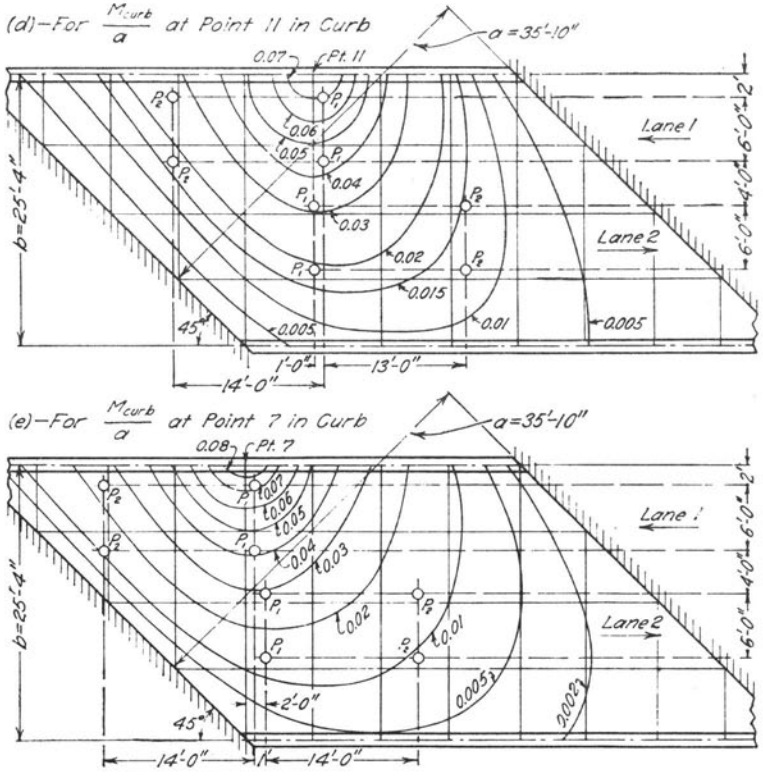

FIG. 18. INFLUENCE SURFACES FOR MOMENTS IN SLAB 45-C
Parts (d) and (e).

TABLE 8

ORDINATES OF INFLUENCE SURFACES FOR MOMENTS IN SLAB 60-B

Data: 60-deg. skew; $b/a = 1.30$; $H = 0.40$; $\mu = 0.2$

The ordinates were computed for the sections at point 11 in the slab and at points 2 and 4 in the curb, as shown in Fig. 1. Contour lines on the influence surfaces are shown in Fig. 19.

Influence Ordinates

Pt.	M_r, pt. 11	M_s, pt. 11	M_{rs}, pt. 11	M_{curb}, pt. 2	M_{curb}, pt. 4
1	0.0191	−0.0175	−0.0036	0.0443 a	0.0012 a
2	0.0366	−0.0306	−0.0069	0.1348 a	0.0183 a
3	0.0208	−0.0161	−0.0029	0.0642 a	0.0086 a
4	0.0403	−0.0268	−0.0094	0.0366 a	0.0970 a
5	0.0494	−0.0234	−0.0042	0.0418 a	0.0570 a
6	0.0313	−0.0130	+0.0004	0.0254 a	0.0262 a
7	0.0621	−0.0008	−0.0112	0.0084 a	0.0250 a
8	0.1052	−0.0038	−0.0014	0.0114 a	0.0252 a
9	0.0609	+0.0008	+0.0090	0.0077 a	0.0146 a
10	0.0959	+0.0745	−0.0005	0.0021 a	0.0075 a
11	0.2629 0.359*	+0.1502 +0.258*	−0.0007	0.0030 a	0.0092 a
10′				0.0021 a	0.0060 a
9′				0.0006 a	0.0024 a
8′				0.0008 a	0.0032 a
7′				0.0006 a	0.0022 a
6′	Ordinates same as for corresponding symmetrical points			0.0001 a	0.0008 a
5′				0.0002 a	0.0012 a
4′				0.0001 a	0.0009 a
3′				0.0000 a	0.0004 a
2′				0.0000 a	0.0006 a
1′				0.0000 a	0.0003 a
	Totals for Dead Load with $q/pa = 0.1290$				
	+0.1436 pa^2	+0.0025 pa^2	−0.0071 pa^2	+0.0439 pa^2	+0.0346 pa^2

* Corrected for wheel load on 1.25-ft. diam. circular area on slab of 19.63-ft. span.

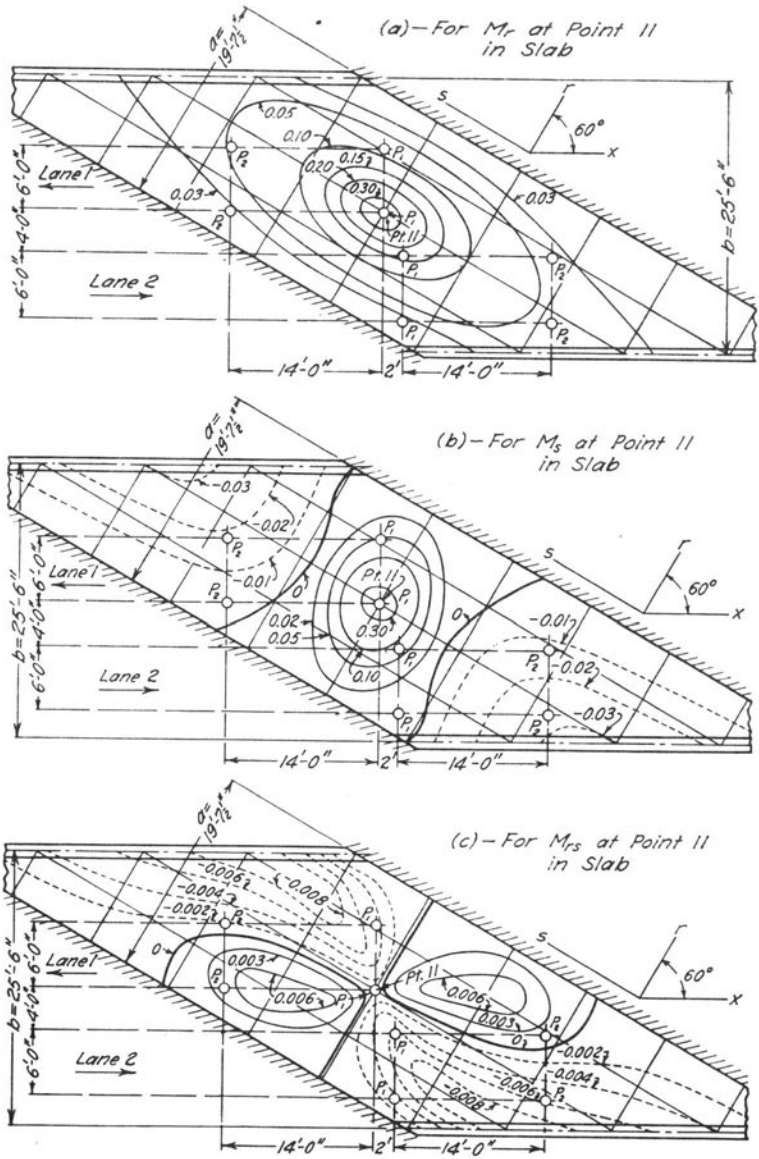

FIG. 19. INFLUENCE SURFACES FOR MOMENTS IN SLAB 60-B

Parts (a) – (c). The figure concludes on page 56.

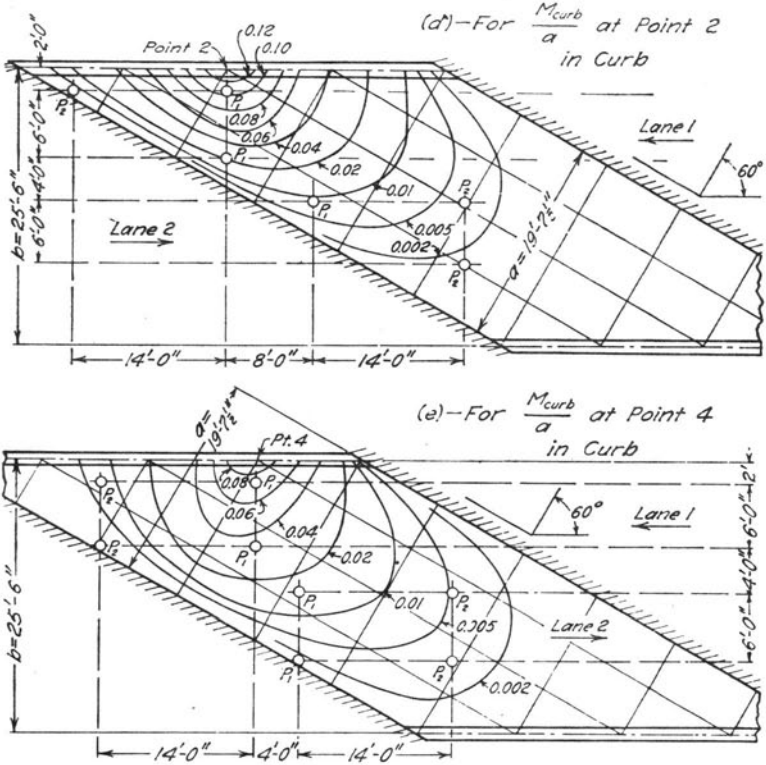

FIG. 19. INFLUENCE SURFACES FOR MOMENTS IN SLAB 60-B
Parts (d) and (e).

TABLE 9

ORDINATES OF INFLUENCE SURFACES FOR MOMENTS IN SLAB 60-C

Data: 60-deg. skew; $b/a = 0.87$; $H = 0.189$; $\mu = 0.2$

The ordinates were computed for the sections at point 18 in the slab and at point 7 in the curb, as shown on Fig. 1. Contour lines on the influence surfaces are shown in Fig. 20.

Influence Ordinates

Pt.	M_r, pt. 18	M_s, pt. 18	M_{rs}, pt. 18	M_{curb}, pt. 7
1	0.0385	−0.0388	−0.0174	0.0046 a
2	0.0769	−0.0742	−0.0343	0.0118 a
3	0.0392	−0.0373	−0.0169	0.0058 a
4	0.1119	−0.0964	−0.0503	0.0291 a
5	0.0808	−0.0653	−0.0310	0.0188 a
6	0.0423	−0.0329	−0.0145	0.0092 a
7	0.1263	−0.0863	−0.0644	0.0786 a
8	0.1254	−0.0684	−0.0420	0.0515 a
9	0.0962	−0.0459	−0.0214	0.0310 a
10	0.0512	−0.0227	−0.0085	0.0146 a
11	0.0854	−0.0322	−0.0550	0.0210 a
12	0.1419	−0.0192	−0.0531	0.0296 a
13	0.1789	−0.0138	−0.0295	0.0272 a
14	0.1300	−0.0028	−0.0049	0.0197 a
15	0.0656	+0.0006	−0.0002	0.0102 a
16	0.0723	+0.0428	−0.0145	0.0069 a
17	0.1627	+0.1010	−0.0209	0.0114 a
18	0.3287 0.408*	+0.1718 +0.263*	−0.0227	0.0122 a
17′				0.0098 a
16′				0.0054 a
15′				0.0027 a
14′				0.0046 a
13′				0.0052 a
12′				0.0043 a
11′				0.0022 a
10′	Ordinates same as for corresponding symmetrical points			0.0011 a
9′				0.0018 a
8′				0.0021 a
7′				0.0016 a
6′				0.0004 a
5′				0.0007 a
4′				0.0007 a
3′				0.0001 a
2′				0.0002 a
1′				0.0001 a
	Totals for Dead Load with $q/pa = 0.0675$			
	+0.1709 pa^2	−0.0381 pa^2	−0.0465 pa^2	+0.0208 pa^2

* Corrected for wheel load on 1.25-ft. diam. circular area on a slab of 29.4-ft. span.

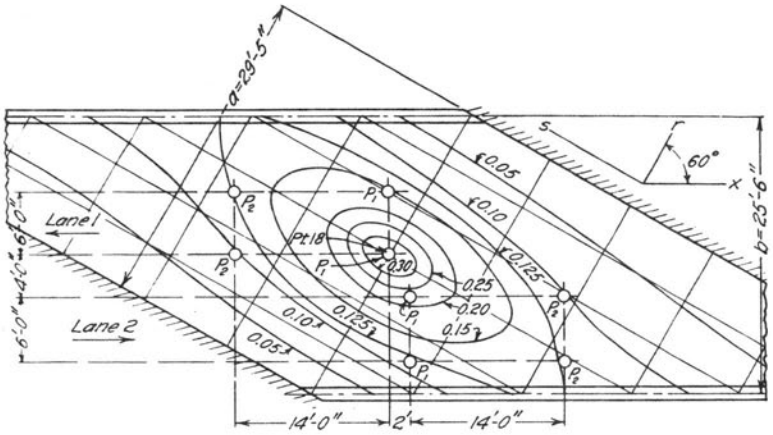

(a)—For M_r at Point 18 in Slab

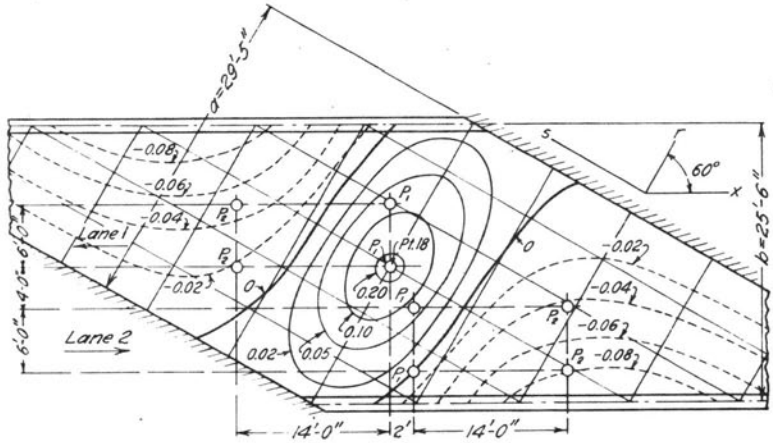

(b)—For M_s at Point 18 in Slab

FIG. 20. INFLUENCE SURFACES FOR MOMENTS IN SLAB 60-C
Parts (a) and (b).

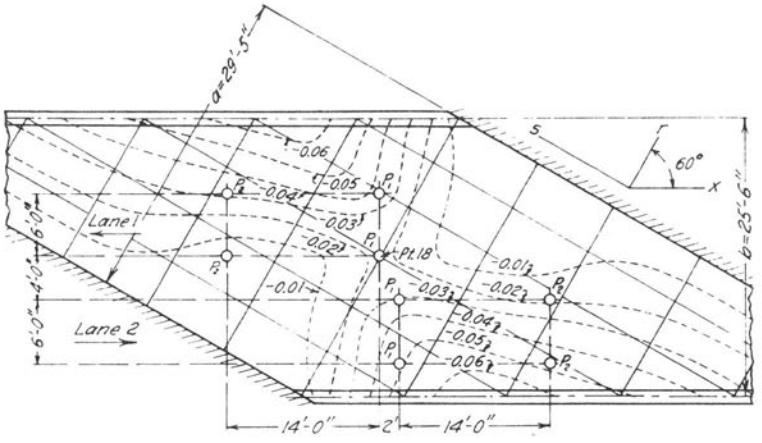

(c)—For M_{rs} at Point 18 in Slab

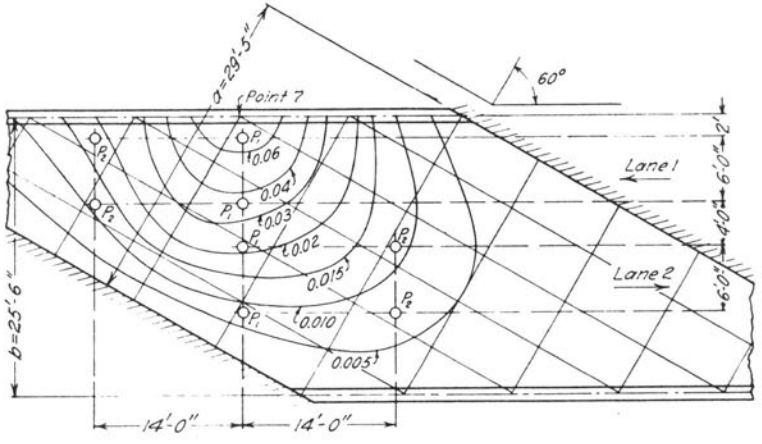

(d)—For $\frac{M_{curb}}{a}$ at Point 7 in Curb

FIG. 20. INFLUENCE SURFACES FOR MOMENTS IN SLAB 60-C
Parts (c) and (d).

APPENDIX C

Moments at the Centers of Skew Slab-Bridges of Short Span

Live load moments at the centers of skew and right bridges have been calculated for bridges having a width center to center of curbs of 25.5 ft. and spans ranging from 2.5 ft. to 10 ft. The results have been used in the text to determine the shape of the curves of live load moment when one or more rear truck wheels are not on the bridge.

It is shown in Bulletin 315 that for the right bridge of b/a ratio greater than 2.8 the moments are practically identical to those in a slab of infinite width. For the skew bridges of short span, all may be considered equivalent to infinite width slabs in so far as the moments at the center are concerned. The procedure in calculation has been to use tables of Bulletin 315 for the comparative right bridges and an influence surface for the infinite strip slab[8] for the skew bridges, both used in conjunction with Westergaard's approximate formulas for moment under a load. Twisting moments have been neglected, since they are small enough to give no appreciable difference between the spanwise and maximum moments or the lateral and minimum moments.

The calculations for maximum and minimum moments are shown without further comment in Figs. 21a and 21b. All values given are for $P = 1$.

[8] H. M. Westergaard, "Computation of Stresses in Bridge Slabs Due to Wheel Loads," Public Roads, Vol. 11, No. 1, p. 15, March, 1930.

$$M_{or} = \frac{1}{2.32 + 8\frac{1.25}{2.5}} = 0.158$$

$$M_{os} = 0.158 - 0.068 = 0.090$$

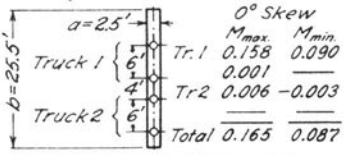

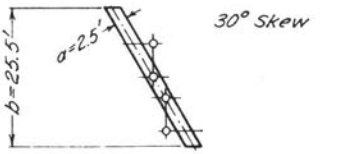

	$M_{max.}$	$M_{min.}$
Truck 1	0.158	0.090
Truck 2	0.004	−0.002
Total	0.162	0.088

$$\frac{0.162 - 0.165}{0.165} = -1.8\%$$

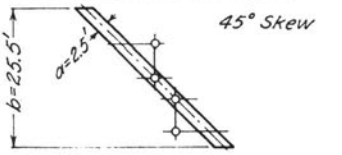

	$M_{max.}$	$M_{min.}$
Truck 1	0.158	0.090
Truck 2	0.002	−0.001
Total	0.160	0.089

$$\frac{0.160 - 0.165}{0.165} = -3.0\%$$

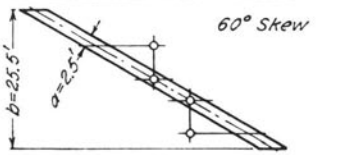

	$M_{max.}$	$M_{min.}$
Truck 1	0.158	0.090
Truck 2	—	—
Total	0.158	0.090

$$\frac{0.158 - 0.165}{0.165} = -4.2\%$$

$$M_{or} = \frac{1}{2.32 + 8\frac{1.25}{5.0}} = 0.231$$

$$M_{os} = 0.231 - 0.068 = 0.163$$

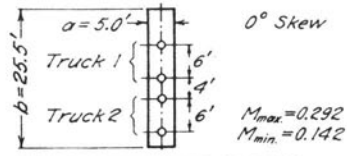

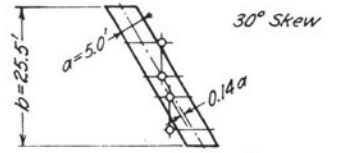

	$M_{max.}$	$M_{min.}$
Truck 1	0.231	0.163
Truck 2	0.037	−0.011
Total	0.268	0.152

$$\frac{0.268 - 0.292}{0.292} = -8.2\%$$

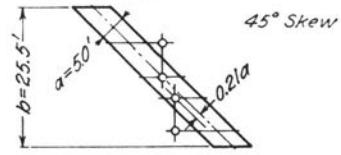

	$M_{max.}$	$M_{min.}$
Truck 1	0.231	0.163
Truck 2	0.026	−0.009
Total	0.257	0.154

$$\frac{0.257 - 0.292}{0.292} = -12.0\%$$

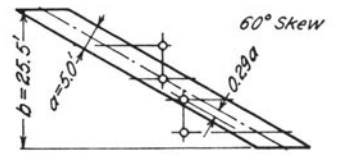

	$M_{max.}$	$M_{min.}$
Truck 1	0.231	0.163
Truck 2	0.013	−0.003
Total	0.244	0.160

$$\frac{0.244 - 0.292}{0.292} = -16.4\%$$

FIG. 21. MOMENTS AT THE CENTER OF SHORT SPAN BRIDGES
Part (a).

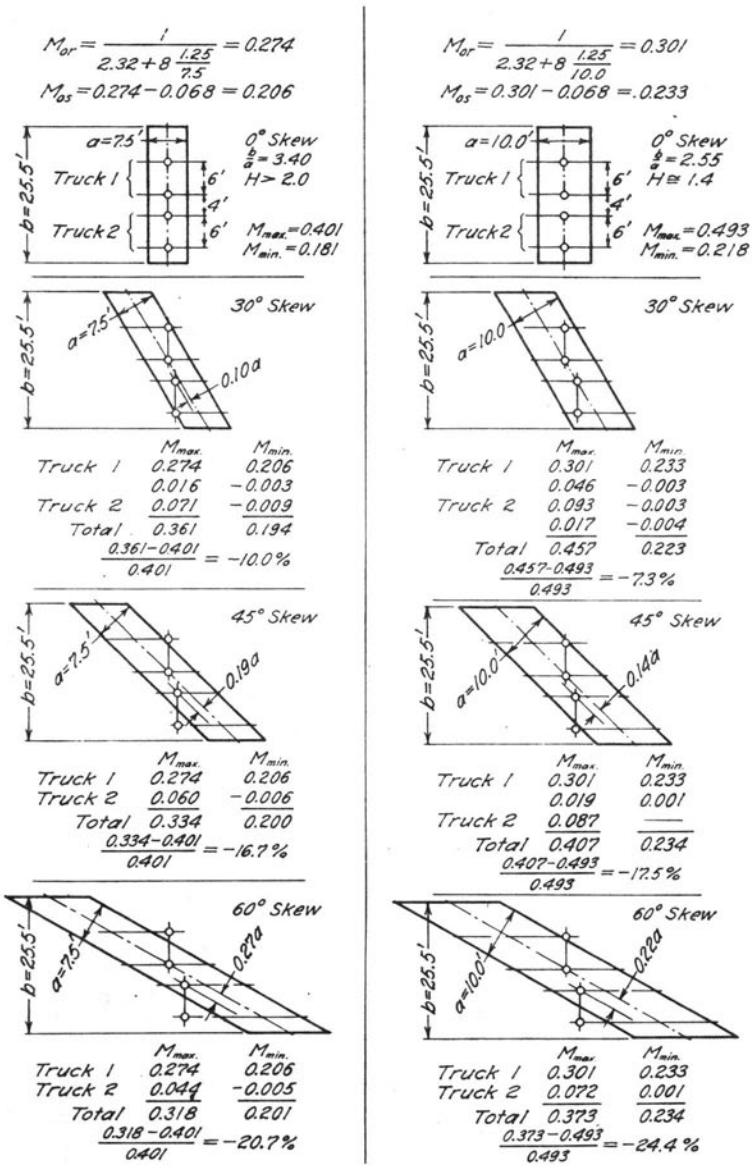

FIG. 21. MOMENTS AT THE CENTER OF SHORT SPAN BRIDGES
Part (b).

Recent Publications of
The Engineering Experiment Station

Bulletins

NO.

338. Influence Charts for Computation of Stresses in Elastic Foundations, by N. M. Newmark. 1942. *Thirty-five cents.*
339. Properties and Applications of Phase-Shifted Rectified Sine Waves, by J. T. Tykociner and L. R. Bloom. 1942. *Sixty cents.*
340. Loss of Head in Flow of Fluids through Various Types of One-and-one-half-inch Valves, by W. M. Lansford. 1942. *Forty cents.*
341. The Effect of Cold Drawing on the Mechanical Properties of Welded Steel Tubing, by W. E. Black. 1942. *Forty cents.*
342. Pressure Losses in Registers and Stackheads in Forced Warm-Air Heating, by A. P. Kratz and S. Konzo. 1942. *Sixty-five cents.*
343. Tests of Composite Timber and Concrete Beams, by F. E. Richart and C. E. Williams, Jr. 1943. *Seventy cents.*
344. Fatigue Tests of Commercial Butt Welds in Structural Steel Plates, by W. M. Wilson, W. H. Bruckner, T. H. McCrackin, Jr., and H. C. Beede. 1943. *One dollar.*
345. Ultimate Strength of Reinforced Concrete Beams as Related to the Plasticity Ratio of Concrete, by V. P. Jensen. 1943. *Seventy cents.*
346. Highway Slab-Bridges with Curbs: Laboratory Tests and Proposed Design Method, by V. P. Jensen, R. W. Kluge, and C. B. Williams, Jr. 1943. *Ninety cents.*
347. Fracture and Ductility of Lead and Lead Alloys for Cable Sheathing, by H. F. Moore and C. W. Dollins. 1943. *Seventy cents.*
348. Fuel Savings Resulting from Closing of Rooms and from Use of a Fireplace, by S. Konzo and W. S. Harris. 1943. *Forty cents.*
349. Performance of a Hot-Water Heating System in the I = B = R Research Home at the University of Illinois, by A. P. Kratz, W. S. Harris, M. K. Fahnestock, and R. J. Martin. 1944. *Seventy-five cents.*
350. Fatigue Strength of Fillet-Weld and Plug-Weld Connections in Steel Structural Members, by W. M. Wilson, W. H. Bruckner, J. E. Duberg, and H. C. Beede. 1944. *One dollar.*
351. Temperature Drop in Ducts for Forced-Air Heating Systems, by A. P. Kratz, S. Konzo, and R. B. Engdahl. 1944. *Sixty-five cents.*
352. Impact on Railway Bridges, by C. T. G. Looney. 1944. *One dollar.*
353. An Analysis of the Motion of a Rigid Body, by E. W. Suppiger. 1944. *Seventy-five cents.*
354. The Viscosity of Gases at High Pressures, by E. W. Comings, B. J. Mayland, and R. S. Egly. 1944. *Seventy-five cents.*
355. Fuel Savings Resulting from Use of Insulation and Storm Windows, by A. P. Kratz and S. Konzo. 1944. *Forty cents.*
356. Heat Emission and Friction Heads of Hot-Water Radiators and Convectors, by F. E. Giesecke and A. P. Kratz. 1945. *Fifty cents.*
357. The Bonding Action of Clays; Part I, Clays in Green Molding Sand, by R. E. Grim and F. L. Cuthbert. 1945. *Free upon request.*
358. A Study of Radiant Baseboard Heating in the I = B = R Research Home, by A. P. Kratz and W. S. Harris. 1945. *Thirty-five cents.*
359. Grain Sizes Produced by Recrystallization and Coalescence in Cold-Rolled Cartridge Brass, by H. L. Walker. 1945. *Free upon request.*
360. Investigation of the Strength of Riveted Joints in Copper Sheets, by W. M. Wilson and A. M. Ozelsel. 1945. *Free upon request.*
361. Residual Stresses in Welded Structures, by W. M. Wilson and Chao-Chien Hao. 1946. *Seventy cents.*
362. The Bonding Action of Clay; Part II—Clays in Dry Molding Sand, by R. E. Grim and F. L. Cuthbert. 1946. *Free upon request.*
363. Studies of Slab and Beam Highway Bridges; Part I—Tests of Simple-Span Right I-Beam Bridges, by N. M. Newmark, C. P. Siess, and R. R. Penman. 1946. *Free upon request.*

Bulletins (Continued)

NO.

364. Steam Turbine Blade Deposits, by F. G. Straub. 1946. *Free upon request.*
365. Experience in Illinois with Joints in Concrete Pavements, by J. S. Crandell, V. L. Glover, W. C. Huntington, J. D. Lindsay, F. E. Richart, and C. C. Wiley. 1946. *In press.*
366. Performance of an Indirect Storage Type of Hot-Water Heater, by A. P. Kratz and W. S. Harris. 1947. *Free upon request.*
367. Influence Charts for Computation of Vertical Displacements in Elastic Foundations, by N. M. Newmark. 1947. *Free upon request.*
368. The Effect of Eccentric Loading, Protective Shells, Slenderness Ratios, and Other Variables in Reinforced Concrete Columns, by F. E. Richart, J. O. Draffin, T. A. Olson, and R. H. Heitman. 1947. *In press.*
369. Studies of Highway Skew Slab-Bridges with Curbs—Part I: Results of Analyses, by V. P. Jensen and J. W. Allen. 1947. *Free upon request.*

Circulars

NO.

42. Papers Presented at the Twenty-eighth Annual Conference on Highway Engineering, held at the University of Illinois March 5-7, 1941. 1942. *Free upon request.*
43. Papers Presented at the Sixth Short Course in Coal Utilization, held at the University of Illinois May 21-23, 1941. 1942. *Free upon request.*
44. Combustion Efficiencies as Related to Performance of Domestic Heating Plants, by A. P. Kratz, S. Konzo, and D. W. Thomson. 1942. *Forty cents.*
45. Simplified Procedure for Selecting Capacities of Duct Systems for Gravity Warm-Air Heating Plants, by A. P. Kratz and S. Konzo. 1942. *Fifty-five cents.*
46. Hand-Firing of Bituminous Coal in the Home, by A. P. Kratz, J. R. Fellows, and J. C. Miles. 1942. *Free upon request.*
47. Save Fuel for Victory. 1942. *Free upon request.*
48. Magnetron Oscillator for Instruction and Research in Microwave Techniques, by J. T. Tykociner and L. R. Bloom. 1944. *Forty cents.*
49. The Drainage of Airports, by W. W. Horner. 1944. *Fifty cents.*
50. Bibliography of Electro-Organic Chemistry, by S. Swann, Jr. 1945. *In press.*
51. Rating Equations for Hand-Fired Warm-Air Furnaces, by A. P. Kratz, S. Konzo, and J. A. Henry. 1945. *Sixty cents.*

Reprints

NO.

28. Tenth Progress Report of the Joint Investigation of Fissures in Railroad Rails, by R. E. Cramer and R. S. Jensen. 1944. *Free upon request.*
29. Second Progress Report of the Investigation of Shelly Spots in Railroad Rails, by R. E. Cramer. 1944. *Free upon request.*
30. Second Progress Report of the Investigation of Fatigue Failures in Rail Joint Bars, by N. J. Alleman. 1944. *Free upon request.*
31. Principles of Heat Treating Steel, by H. L. Walker. 1944. *Fifteen cents.*
32. Progress Reports of Investigation of Railroad Rails and Joint Bars, by H. F. Moore, R. E. Cramer, N. J. Alleman, and R. S. Jensen. 1945. *Free upon request.*
33. Progress Report on the Effect of the Ratio of Wheel Diameter to Wheel Load on Extent of Rail Damage, by N. J. Alleman. 1945. *Fifteen cents.*
34. Progress Report of the Joint Investigation of Methods of Roadbed Stabilization, by R. B. Peck. 1946. *Free upon request.*
35. Progress Reports of Investigation of Railroad Rails and Joint Bars, by R. E. Cramer, N. J. Alleman, and R. S. Jensen. 1946. *Free upon request.*
36. Electro-Organic Chemical Preparations: Part III, by S. Swann, Jr. 1947. *Free upon request.*
37. Progress Reports of Investigation of Railroad Rails and Joint Bars, by R. E. Cramer, N. J. Alleman, and R. S. Jensen. 1947. *Free upon request.*
38. Second Progress Report of the Joint Investigation of Methods of Roadbed Stabilization, by R. B. Peck. 1947. *Free upon request.*

UNIVERSITY OF ILLINOIS

Divisions of Instruction

Institute of Aeronautics
College of Agriculture
College of Commerce and Business Administration
College of Dentistry
College of Education
College of Engineering
College of Fine and Applied Arts
Graduate School
School of Journalism
Institute of Labor and Industrial Relations
College of Law
College of Liberal Arts and Sciences
Library School
College of Medicine
Department of Military Science and Tactics
Department of Naval Science
College of Pharmacy
School of Physical Education
Division of Social Welfare Administration
Division of Special Services for War Veterans
Summer Session
University Extension Division
College of Veterinary Medicine

University Experiment Stations and Research and Service Organizations at Urbana

Agricultural Experiment Station
Bureau of Community Planning
Bureau of Economic and Business Research
Bureau of Institutional Research
Bureau of Research and Service
Engineering Experiment Station
Extension Service in Agriculture and Home Economics
General Placement Bureau
High School Testing Bureau
Radio Station (W I L L)
Services for Crippled Children
Small Homes Council
Student Personnel Bureau
University of Illinois Press

State Scientific Surveys and Other Divisions at Urbana

State Geological Survey
State Natural History Survey
State Water Survey
State Diagnostic Laboratory (for Animal Pathology)
U. S. Regional Soybean Laboratory

For general catalog of the University, special circulars, and other information, address The Director of Admissions and Records, University of Illinois, Urbana, Illinois